



FINAL REPORT

AROMATIC ORGANIC LASER DEVELOPMENT

by
DL Stockman

COPY	2	OF	3
MADE COPY			\$. 3. 00
MICROFILM			\$. 0. 75

76P

This research is part of PROJECT DEFENDER under the joint sponsorship of the Advanced Research Projects Agency, the Office of Naval Research and the Department of Defense.

Contract No. NONR 4135 (00)
From Office of Naval Research
Project Code 3730
Order No. 306-62

Prepared for
Office of Naval Research
Department of the Navy
Washington 25, D.C.

Prepared by

Electronics Laboratory
General Electric Company
Electronics Park
Syracuse, New York

Submitted by

Heavy Military Electronics Dept.
General Electric Company
Building 3, Room 4
Court Street
Syracuse, New York

ARCHIVE COPY

**BEST
AVAILABLE COPY**

Final Report

AROMATIC ORGANIC LASER DEVELOPMENT

Contract No. NONR 413500
from the
Office of Naval Research

Sponsored by

Advanced Research Projects Agency
Project Code 3730
Order No. 306-62

Contract Initiation Date: 1 April 1963
Contract Termination Date: 31 March 1965
Amount of Contract: \$90,314.00

Prepared by

Electronics Laboratory
General Electric Company
Electronics Park
Syracuse, New York
992-GH-921

Submitted by

Heavy Military Electronics Dept.
General Electric Company
Bldg. 3, Room 4
Court Street
Syracuse, New York

TABLE OF CONTENTS

<u>Section</u>		<u>Page</u>
I	INTRODUCTION AND SUMMARY.....	1
II	THEORETICAL CONSIDERATIONS.....	2
	A. Introduction.....	2
	B. Spontaneous Emission in Aromatic Organic Compounds	2
	C. Oscillation Conditions for the Resonant Cavity....	4
	D. Conclusions.....	12
III	MATERIALS SELECTION AND PREPARATION.....	13
	A. Fluorescent Compounds and Their Properties.....	13
	B. Preparation of Liquid Samples.....	30
	C. Selection of Plastic Hosts and Their Preparation..	30
IV	DEVICE CONSIDERATIONS.....	48
	A. Optical Pumping Systems.....	48
	B. Fabry-Perot and Confocal Resonant Cavities.....	64
V	RESULTS OF OPTICAL PUMPING EXPERIMENTS.....	65
VI	APPENDIX - Preparation of Ceramic Capacitors.....	69
VII	BIBLIOGRAPHY.....	71
VIII	DISTRIBUTION LIST.....	73

LIST OF FIGURES

Figure No.		Page No.
1	A Modified Jablonski Diagram for an Aromatic Hydrocarbon	3
2.	Possible Stimulated Emission Mechanisms in Organic Molecules	6
3.	Absorption and Fluorescence Spectrum of Perylene in Benzene	10
4.	Absorption and Fluorescence Spectrum of Perylene in PMMA-10.5% DBP	15
5.	Long Wavelength Absorption of Perylene in Benzene	17
6.	Absorption and Fluorescence Spectrum of 9-Aminoacridine in H ₂ O	18
7.	Absorption and Fluorescence of 9-Aminoacridine in PMMA-10.5% DBP	20
8.	Absorption and Fluorescence of 9,10-Diphenylanthracene in Isooctane	21
9.	Absorption and Fluorescence of 9,10-Diphenylanthracene in PMMA-10.5% DBP	22
10.	Absorption and Fluorescence of 9-methylanthracene in Hexane	24
11.	Absorption and Fluorescence of 9-methylanthracene in PMMA-10.5% DBP	25
12.	Absorption and Fluorescence of Rubrene in Hexane	26
13.	Absorption and Fluorescence of Rubrene in PMMA-10.5% DBP	27
14.	Fluorescence Spectrum of Single Crystal Anthracene and Single Crystal Anthracene 10 ⁻³ m Naphthacene	29
15.	Stress-Optical Coefficient of PMMA as a Function of DBP Concentration	37
16.	Expansion Rate of PMMA-10.5% DBP as a Function of Temperature	39
17.	Refractive Index of PMMA-10.5% DBP as a Function of Wavelength	42
18.	Ultraviolet Absorption of PMMA-10.5% DBP	43
19.	Expansion of PMMA-10.5% DBP as a Function of Temperature	44
20.	Optical Quality of PMMA-10.5% DBP-Interference and Polarization	46
21.	Photograph of Experimental Xenon Lamp	49
22.	Photograph of Argon Theta Pinch Lamp	54
23--25.	Spectral Output of Argon Theta Pinch Lamp	56-58
26.	Time Dependent Output of Various Species in Argon Theta-Pinch Lamp	62
27.	Optical System for Fluorescence Gain Measurements	66
28.	Fluorescence of Perylene in Benzene Solution at Various Wavelengths	67

I. INTRODUCTION AND SUMMARY

The purpose of this program has been to produce coherent stimulated emission in the blue-green region in a purely organic dopant and host system. Toward this end, a theoretical analysis of the problem has been made and experimental work on the development of such a laser has been done.

The theoretical analysis indicates that the short lived ($\tau \sim 10^{-8}$ seconds) four-level fluorescent compounds are the most suitable materials for this purpose. A total of four fluorescent compounds were found with the appropriate spectroscopic characteristics. Phosphorescent compounds, with lifetimes in the range 10^{-3} - 10^1 seconds, show little immediate promise because of high internal loss mechanisms in addition to their poor spontaneous emission characteristics.

The principal experimental difficulties have included the development of a suitable host material in which the absorbing and scattering losses are kept to a minimum and an optical pump system capable of efficiently producing several megawatts of absorbable peak power in a short time. An optically isotropic polymer was developed whose properties appear to be suitable as a host material for the fluorescing species. Liquid hosts were also used in the early part of the program. Two optical pumping systems were used: (1) a modified Xenon lamp, and (2) an argon theta-pinch lamp. Both of these systems were used to pump the samples. Some gain was observed in a liquid containing perylene as the active compound. This gain was observed at 4710 Å and probably was due to preoscillation "superradiance." Gain in the fluorescent compounds contained in the polymer rods was not observed.

This report is divided into four major segments which includes the theoretical analysis, materials selection and preparation, device development, and experimental pumping results.

II. THEORETICAL CONSIDERATIONS

A. Introduction

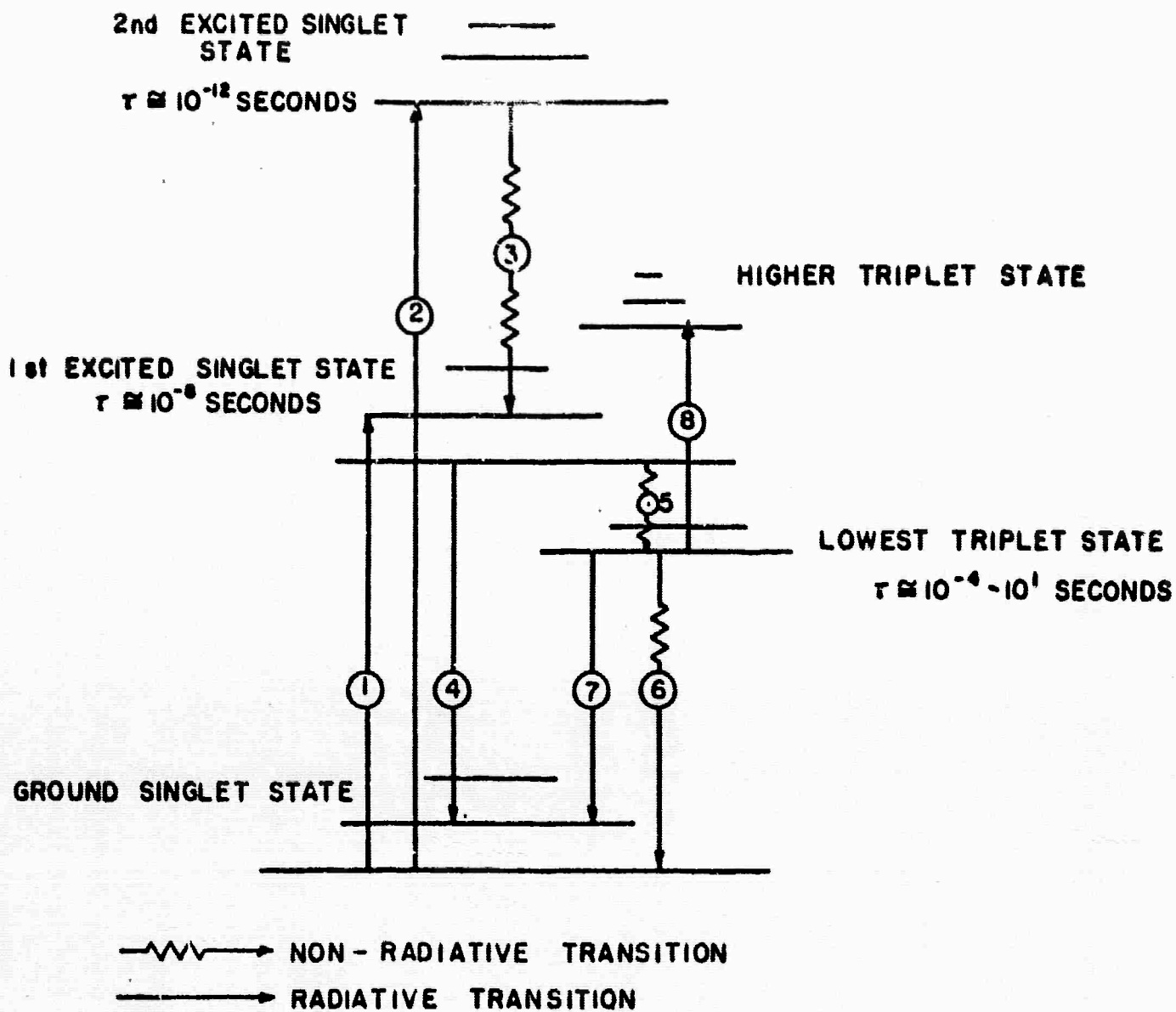
The first suggestion of the use of organic compounds for producing coherent stimulated emission was made by Brock, et.al.⁽¹⁾ The possibility of population inversion in organic compounds had been treated theoretically earlier by Ivanov⁽²⁾. Subsequently, Morantz and coworkers⁽³⁻⁵⁾, reported the observation of phenomena in the phosphorescence of several systems which they attributed to stimulated emission. Lempicki and Samelson⁽⁶⁾, Wilkinson and Smith⁽⁷⁾, and Stockman⁽⁸⁾, have questioned these results both from an experimental and a theoretical point of view.

We shall first be concerned with some general observations on the various spontaneous emissions occurring in organic compounds and then shall qualitatively consider their potential to produce coherent stimulated emission in practical systems.

B. Spontaneous Emission in Aromatic Organic Compounds

Aromatic organic molecules have some electrons which are delocalized over the entire structure of the molecule. The electronic transitions involving these delocalized electrons occur mainly in the visible and near ultraviolet regions of the spectrum. The spectra are broadened due to the large number of vibrational and rotational sublevels within each electronic state. The various excited states and their relationships for an aromatic hydrocarbon (where only $\pi-\pi^*$ transitions exist) can be understood qualitatively by the modified Jablonski diagram in Figure 1.

Absorption of light (transitions 1 and 2 in Figure 1) takes the molecule from the ground singlet state to the higher singlet states. The absorption cross sections for these transitions can be very high ($\sim 10^{-16}$ cm²/molecule). If excitation is to the second excited singlet state, a non-radiative internal conversion (transition 3) places the molecule in the first excited singlet state. In this state, the molecule quickly ($\sim 10^{-12}$ seconds) reaches thermal equilibrium with its surroundings. The



A MODIFIED JABLONSKI DIAGRAM FOR AN AROMATIC HYDROCARBON
 FIGURE 1

subsequent non-radiative and emission processes which will eventually take place are determined at this time when the molecule either fluoresces (transition 4) ($\tau \sim 10^{-8}$ seconds) or undergoes an "intersystem crossing" (transition 5)⁽⁹⁾ to the lowest triplet state of the molecule. For an aromatic hydrocarbon, such as anthracene, these two processes have comparable rates. In compounds such as benzophenone (where the $n-\pi^*$ transitions are also present), "intersystem crossing" to the triplet state generally predominates. The triplet state is rather long lived and in fluid solvents collisional deactivation (transition 6) occurs with no significant emission being observed. In rigid media, however, a long lived emission (10^{-4} - 10^1 seconds) is observed (transition 7) and this emission is termed phosphorescence.

A third type of emission which has the spectrum of a fluorescence and the lifetime of a triplet state is also observed in some compounds. In such systems it has been shown that the triplet state and the excited singlet state are very close in energy and that thermal recrossing from the triplet to the singlet state occurs followed by the fluorescence emission. This emission is termed α -phosphorescence or long-lived fluorescence⁽¹⁰⁾.

One more important transition deserves mention. Molecules also possess higher triplet states. If a significant fraction of the molecules are in the lowest triplet state, a high triplet-triplet absorption can be observed (transition 8). In some molecules these transitions are relatively sharp, but in most molecules they are extremely broad, sometimes extending over the entire visible wave length region. This process will be one of the most important limiting factors for the application of phosphorescent systems to the generation of coherent stimulated emission. These processes are discussed in more detail elsewhere⁽¹⁰⁻¹²⁾.

C. Oscillation Conditions in an Optical Cavity Employing Organic Compounds

In this section we will consider the potential of the fluorescent and phosphorescent molecules to undergo oscillation in a resonant cavity under stimulated emission conditions. The postulated schematic representation of

each mechanism is shown in Figure 2. In addition, we shall calculate the power gain anticipated above threshold which will give a measure of the expected usefulness of the material. We shall follow the procedure of Yariv and Gordon⁽¹³⁾ although the rate equation approach of Maiman⁽¹⁴⁾ yields essentially the same results.

We use as the "start-oscillation" condition that

$$\frac{\Delta N_{32}}{V} = \frac{8\pi \nu^2 \tau_0}{c^3 g(\nu_c) \tau_{\text{photon}}}, \quad (1)$$

where $\Delta N_{32}/V$ is the concentration difference between levels 3 and 2 (see Figure 2), per unit volume, and τ_0 is the intrinsic mean radiative lifetime. τ_0 is related to the observed mean lifetime, τ_3 , by

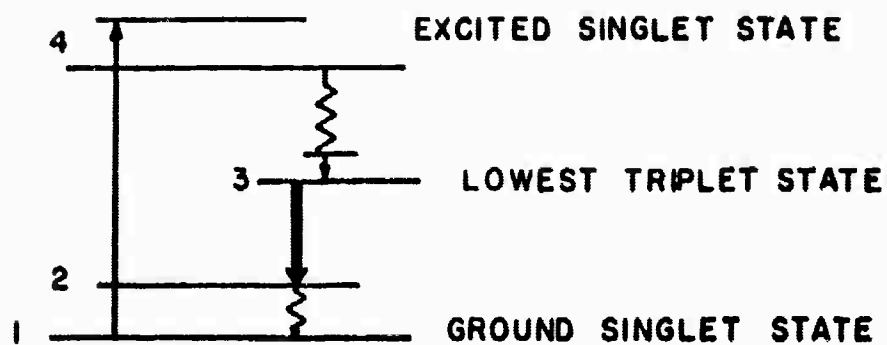
$$\phi = \frac{\tau_3}{\tau_0}$$

where ϕ is the quantum efficiency. τ_{photon} is the decay time constant of the radiation in a given mode if the amplifying medium is rendered neutral, i.e., $\Delta N_{32} = 0$. It thus contains all parameters relating to an experimental cavity. It is given by

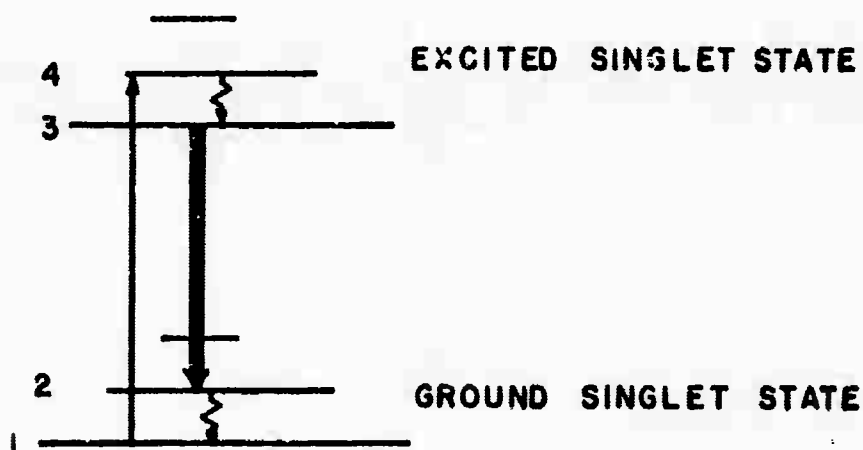
$$\tau_{\text{photon}} = \frac{L}{\alpha c}, \quad (2)$$

where L is the length of the cavity, c is the speed of light in the medium, and α is the total loss per pass in the material (including optical scattering losses, reflection losses, diffraction losses, absorption losses, if any, and mirror losses). This expression is valid if $\alpha \ll 1$. Equation 1 also contains the frequency dependence of the spontaneous emission band $g(\nu)$. For a Gaussian emission line,

$$g(\nu_c) = \frac{2(\pi \ln 2)^{\frac{1}{2}}}{\pi \Delta \nu}, \quad (3)$$



a.) STIMULATED EMISSION VIA PHOSPHORESCENCE



b.) STIMULATED EMISSION VIA FLUORESCENCE

POSSIBLE STIMULATED EMISSION MECHANISMS IN ORGANIC MOLECULES.

FIGURE 2

where $\Delta \nu$ is the full width at half maximum and ν_c is the center frequency. Substituting (2) and (3) in (1), and converting to frequency in wave numbers, $\omega = \frac{\nu}{c}$,

$$\frac{\Delta N_{32}}{\nu} = \frac{4\pi^2 c \omega^2 \Delta \omega \tau_0}{(\pi \ln 2)^2 L} \quad (4)$$

For a four level system where $\Delta E_{21} \gg kT$, then $\frac{\Delta N_{32}}{\nu}$ is an accurate measure of the number of molecules required in the system for the onset of oscillations under the specified loss conditions. For a three level system, of course,

$$\Delta N (\text{total}) = \frac{1}{2} \left[N_0 + \Delta N_{32} \right] \quad (5)$$

where N_0 is the total number of molecules present.

The power gain per unit length, γ , can be shown to be⁽¹³⁾

$$\gamma = \frac{(\pi \ln 2)^2 \left(\frac{\Delta N}{\nu} \right)_{\text{excess}}}{4 \pi^2 \omega^2 c \Delta \omega \tau_0} \quad (6)$$

This power gain does not depend on whether the system is three or four level since the oscillation threshold is reached, the power gain depends only on the excess concentration above threshold. We will now apply these equations to particular systems.

Case A - Phosphorescent Molecules

We will take as a favorable case the molecule benzophenone. Others have been considered elsewhere⁽⁷⁾. The absorption region of this compound is around 2500 - 3000 Å. A phosphorescence lifetime $\tau_3 = 4.5 \times 10^{-3}$ seconds ($\phi = 0.84$) is observed⁽¹⁵⁾ with several emission bands. The most intense band is located (in a isopentane methylcyclohexane glass) at 22,500 cm^{-1} .

$\Delta \omega$ (for this band) is 1200 cm^{-1} . We will use a refractive index = 1.5 and a loss of 0.18 per pass in a 6 cm. long cell, assuming that scattering is the major contributing loss mechanism which at 1.06 microns was found to be 3% per cm. Substituting into equation 4, the critical concentration density is

$$\frac{\Delta N_{32}}{V} = 6.5 \times 10^{19} \text{ molecules/cm}^3 .$$

This calculation assumes that all of the phosphorescence is in the $22,500 \text{ cm}^{-1}$ band. Since only 25% of the total phosphorescence is within the $22,500 \text{ cm}^{-1}$ band, this calculated concentration must be increased by a factor of 4. This value is the actual inversion density required since this system is a four level system with $\Delta E_{21} \sim 1500 \text{ cm}^{-1}$ (the location of the highest frequency phosphorescence peak is at $\sim 24,000 \text{ cm}^{-1}$). From the above calculation, it is seen that a very high concentration is needed just to overcome reasonably low losses. In any practical organic glass system at 77°K , the optical system will be more complex, which will increase the losses even further.

In addition, this calculation has assumed that no absorption loss will be present for this system. In fact, this is not true. The triplet-triplet absorption of benzophenone has been measured by Porter and Windsor⁽¹⁶⁾. From this measurement, we estimate the absorption cross section σ (at $22,500 \text{ cm}^{-1}$) $\geq 10^{-18} \text{ cm}^2/\text{molecule}$. There is an additional relative loss corresponding to σN_3 per cm. At the calculated concentration of about 10^{20} molecules/cc, this would be the predominant loss*. This loss mechanism should manifest itself by a saturation of the spontaneous phosphorescent intensity under high excitation intensities. Such behavior for benzophenone has been observed recently⁽¹⁷⁾.

The power gain factor for such a phosphorescent system can be calculated from equation 6, for benzophenone, to be

* In this instance the equations given above are not valid since the total loss per pass, α , must now be expressed with an exponential dependence for the losses on concentration.

$$\gamma = 5.7 \times 10^{-22} \left(\frac{\Delta N}{V} \right)_{\text{excess phosp}}$$

A comparison with ruby is illustrative. For ruby the following factors are used⁽¹⁴⁾ (a Gaussian emission line assumed).

$\lambda = 6943 \text{ \AA}$, $\omega = 1.44 \times 10^4 \text{ cm}^{-1}$, $\tau = 3 \times 10^{-3}$ seconds, $\Delta \omega = 11 \text{ cm}^{-1}$, $n = 1.76$. Therefore,

$$\gamma_{\text{ruby}} = 3.3 \times 10^{-19} \left(\frac{\Delta N}{V} \right)_{\text{excess ruby}}$$

Now let us assume that we desire the same gain factor as for ruby for a reasonable resonant cavity gain. The ratio of the excess concentration of the phosphorescent compound to the ruby excess concentration over that required for threshold is seen to be

$$\frac{\left(\frac{\Delta N}{V} \right)_{\text{excess phosp}}}{\left(\frac{\Delta N}{V} \right)_{\text{excess ruby}}} = \frac{3.3 \times 10^{-19}}{5.7 \times 10^{-22}} = 580$$

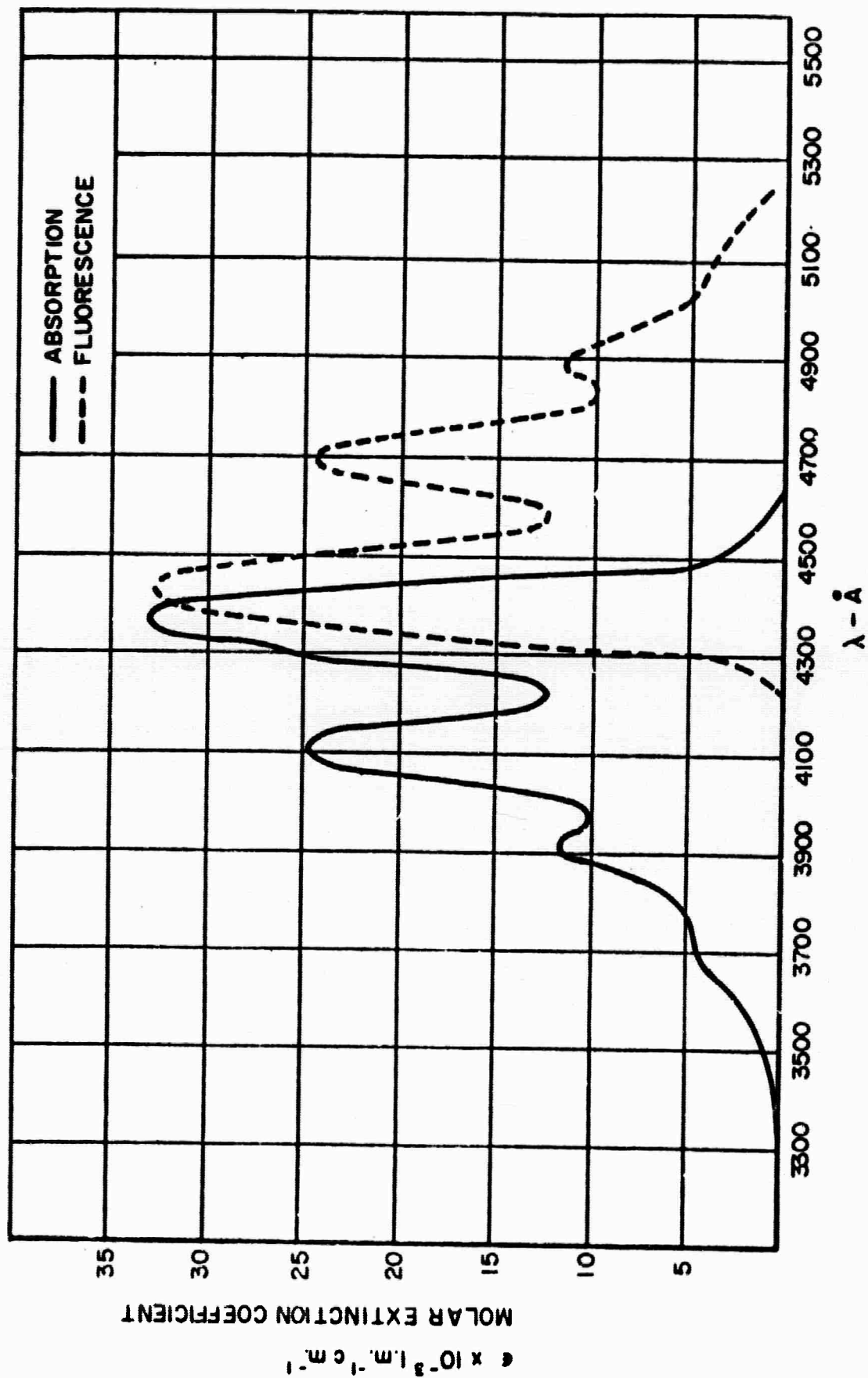
Therefore, we need large increases in concentration over ruby to produce the same gain above threshold in a phosphorescent system. This implies a very low potential power gain for these compounds, due principally to the difference in the emission band width.

Case B - Fluorescent Compounds

For the typical four level fluorescent case, we will use the molecule perylene. The absorption and fluorescence spectrum for perylene in benzene at 25°C is shown in Figure 3. The following data have been obtained (see Section III) here and elsewhere⁽¹⁸⁾.

$\lambda = 4710 \text{ \AA}$, $\omega = 2.12 \times 10^4 \text{ cm}^{-1}$, $\Delta \omega = 800 \text{ cm}^{-1}$ (for the 4700 Å band), $\tau_0 = 6.9 \times 10^{-9}$ seconds (with $\phi = 0.96$), and, as before, $n_D = 1.5$, $L = 6 \text{ cm}$ and $\alpha = 0.18$. Substituting into (4), the critical inversion concentration is

$$\frac{\Delta N_{32}}{V} = 4.3 \times 10^{13} \text{ molecules/cm}^3$$



ABSORPTION AND FLUORESCENCE SPECTRUM OF PERYLENE IN BENZENE

FIGURE 3

This calculation assumes all radiation is in the $21,200 \text{ cm}^{-1}$ band whereas only one-third is actually there (see Figure 3). Therefore, the actual number required must be increased threefold to 1.3×10^{14} molecules/cm³. Because of the low required inversion population, the thermal population of the terminal state may be important. The perylene molecule is, of course, not an exact 4-level fluorescent system. The terminal-ground state separation is 1500 cm^{-1} which means that a solution containing a total concentration of 6×10^{16} molecules/cm³ (1×10^{-4} moles/liter) would have 4.7×10^{13} molecules/cm³ in the terminal state at room temperature. This amount must be added to that calculated alone to the losses giving a total required population of about 1.7×10^{14} molecules/cm³.

The critical or minimum pump power required for this system to oscillate is given by

$$P_{th} = \frac{\Delta N_{total} h\bar{\nu}_{pump}}{V \tau_0} = 1.25 \times 10^4 \text{ watts/cm}^3.$$

where $h\bar{\nu}_{pump} = 5 \times 10^{-19}$ joules/photon, where P_{th} is the pump power required at the surface of the material which is capable of being absorbed. For our Xenon lamp pump systems, the luminous efficiency is about 10% with about 10% of the output radiation within the band of the absorption of perylene for an (minimum) equivalent black body temperature of 6000°K . Assuming a coupling and absorbing efficiency of 50%, the overall electrical pump power requirement is

$$P_{electrical} = 1.25 \times 10^4 \times 10 \times 10 \times 2 = 2.5 \times 10^6 \text{ watts/cm}^3.$$

For a 3 cc volume, with the pump pulse duration of the order of 10^{-6} seconds, the electrical energy input is seen to be approximately 7.5 joules. Due to many assumptions employed, it is possible that this estimate could be too low by one order of magnitude. (For a three-level fluorescent system, the pump power requirements are obviously much higher and probably cannot be attained with presently available pumping systems.)

The power gain for this four level fluorescent system can also be calculated. Using the same numbers as above for perylene, the ratio of

excess concentrations is seen to be (when the power gain is the same),

$$\frac{\left(\frac{\Delta N}{V}\right)_{\text{excess fluor}}}{\left(\frac{\Delta N}{V}\right)_{\text{excess ruby}}} = \frac{3.3 \times 10^{-19}}{7.4 \times 10^{-17}} = 1.3 \times 10^{-3} .$$

This implies a relatively low concentration to produce comparable gain above threshold and indicates that high power gains could be anticipated.

C. Conclusions

On the basis of the foregoing considerations, it is concluded that the four-level fluorescent systems offer the most potential for the production of coherent stimulated emission, in spite of the high peak power required from an optical pump. Accordingly, the experimental program has concentrated entirely on this type of compound. Calculations on the other compounds chosen for this study (see Section III) give qualitatively similar results. Certain phosphorescent compounds might be found whose line width, triplet-triplet absorption and spontaneous lifetimes would be more favorable and they should then be considered for device development.

III. MATERIALS SELECTION AND PREPARATION

A. Fluorescent Compounds and Their Properties

The choice of a suitable fluorescent compound rests on the following general considerations:

1. The spectroscopy of the molecule should indicate at least a pseudo four-level system as indicated in Figure 2.
2. The quantum yield of fluorescence should be very nearly unity to prevent build up of the triplet state due to multiple pumping (see Section V).
3. The compound should be relatively insensitive to excimer (excited dimer) formation so that reasonably high concentrations can be used in trying different host materials and in using different configurations.
4. The absorption of the molecule should be at wavelengths higher than about 3400 Å in order that they may be evaluated in state-of-the-art optical quality plastic hosts, whose absorption begins at about 3400 Å.

A large number of potential compounds were screened for their application as laser materials. The most promising compounds are:

1. Perylene.
2. 9-Aminoacridine.
3. 9,10-Diphenylanthracene.
4. 9-Methylanthracene
5. Rubrene (9,10,11,12-Tetraphenyl-naphthacene)
6. Naphthacene in an anthracene crystal.

1. Perylene

Perylenes' absorption and emission spectrum in benzene at room temperature was shown in Figure 3. The quantum efficiency, ϕ , and measured mean life time, τ are related to the intrinsic mean life time τ_0 ,

(calculated from the measured absorption data) by

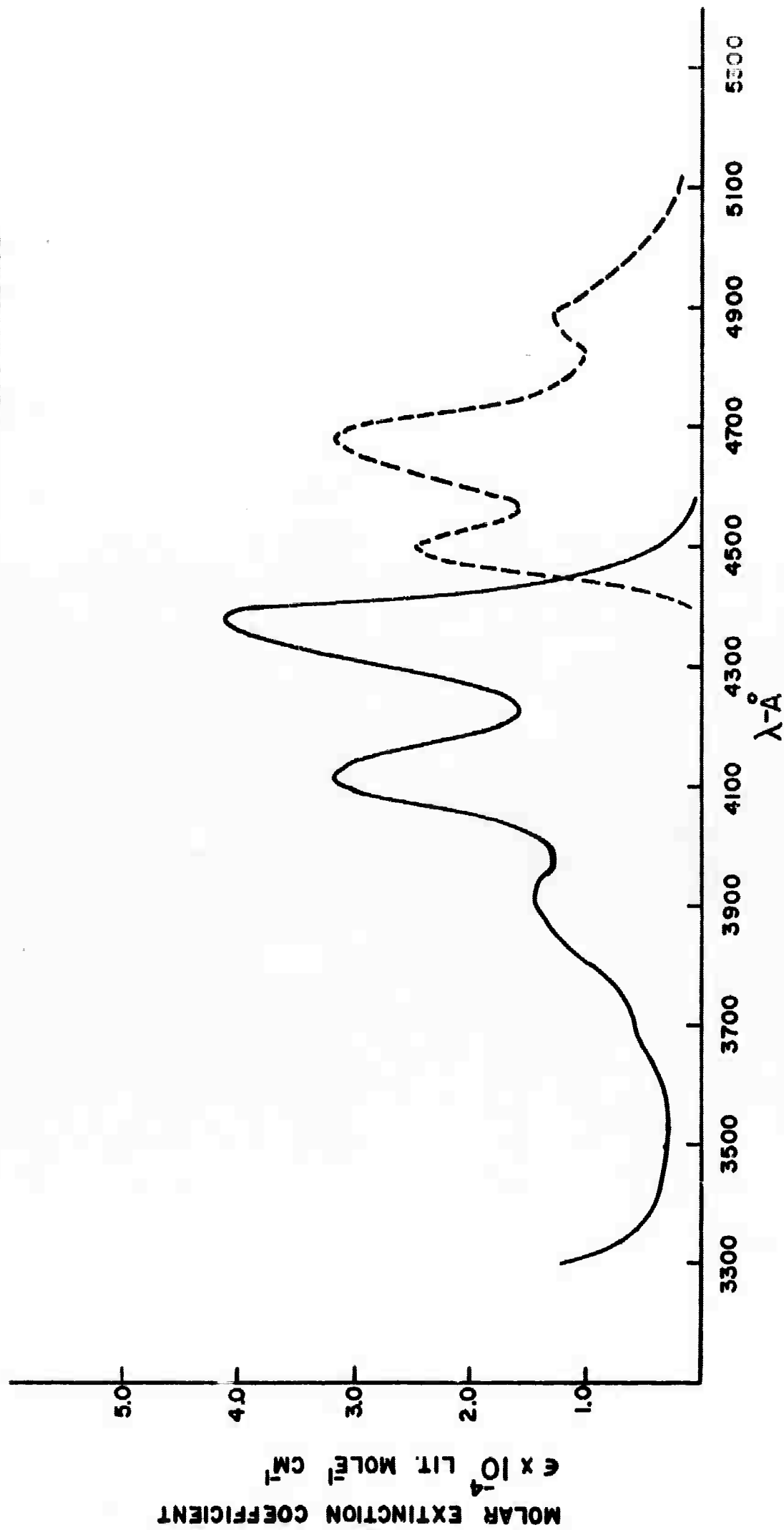
$$\phi = \frac{\tau}{\tau_0}$$

Livingston and Bowen⁽¹⁸⁾ report a quantum efficiency, for perylene in benzene of 0.96 with $\tau = 6.9 \times 10^{-9}$ seconds whereas Strickler and Berg⁽¹⁹⁾ measure $\tau = 4.8 \times 10^{-9}$ seconds with a quantum efficiency of 1. The difference may be due in the difference in determination of . Livingston and Bowen measured the quantum efficiency and calculated from the absorption spectrum, not taking into account the frequency change between absorption and emission. Strickler and Berg did take the shift into account and measured the decay time directly by phase shift measurements. The quantum efficiency in the plastic host is not measurably different from unity.

The perylene molecule is photochemically stable in various hosts under high excitation intensities in the absence of dissolved oxygen. It thus meets all of the requirements. The line most suitable for amplification in this molecule is the fluorescent band centered at 4710 Å, although the 4900 Å band in principle could also be used with correspondingly lower gain. The band at 4450 Å is not suitable since it represents a three-level fluorescence. The temperature dependence of the spectra has been discussed elsewhere⁽²⁰⁾, but there is nothing to be gained by lowering the temperature either in the plastic or benzene host. The absorption of perylene in the modified polymethyl methacrylate host (see Section III-C) is shown in Figure 4. The short wavelength fluorescence band has undergone partial re-absorption due to the fact that the fluorescence was measured on a 2×10^{-5} m perylene concentration sample rather than on an optically thin sample (1×10^{-6} m) as done with the solutions. The four-level fluorescence peak is located at $4684 \text{ Å} \pm 1 \text{ Å}$ as compared to 4710 Å when in the benzene solution.

The long wavelength absorption of perylene in benzene was measured in order to determine if the Boltzman population of the terminal state at 4710 Å was in agreement with the computed values

— ABSORPTION
- - - FLUORESCENCE



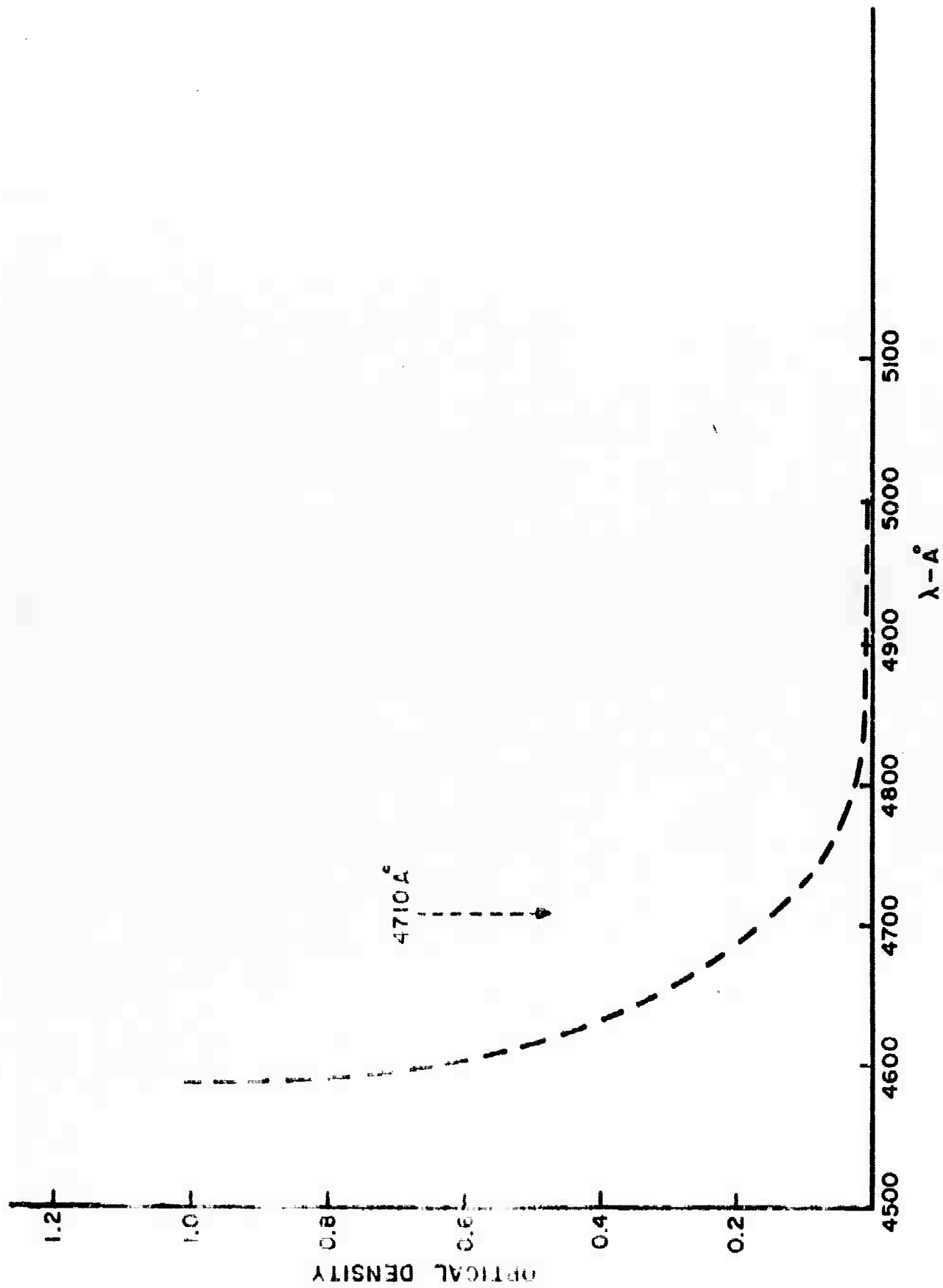
ABSORPTION AND FLUORESCENCE OF PERYLENE IN PMMA-10.5% DBP
FIGURE 4

based on the spectroscopic observations. From the absorption and emission data for perylene, shown in Figure 3, the terminal-ground state splitting is measured by the energy difference between the 4710 Å fluorescence peak and the cross-over (the 0-0 transition) point between the absorption and emission spectrum at 4445 Å. The energy separation is $1266 \pm 20 \text{ cm}^{-1}$. The long wavelength absorption ($> 4445 \text{ Å}$) of the perylene is due to transitions of the upper vibrational-rotational levels of the ground electronic state to the lowest vibrational-rotational level of the excited state. The population arises from simple Boltzmann statistics. Owing to the near perfect mirror symmetry of the absorption and fluorescence spectrum, it would be anticipated that absorption at the 4710 Å terminal state would have the approximately same cross section as the 4100 Å absorption peak.

Figure 5 illustrates the experimentally obtained absorption of a 5.56×10^{-4} molar solution of perylene in benzene using a 10 cm. cell. From the optical density at 4710 Å, we calculate that the terminal ground state separation is about 1300 cm^{-1} in fair agreement with the spectroscopic value. Due to the assumptions employed, no better agreement should be expected.

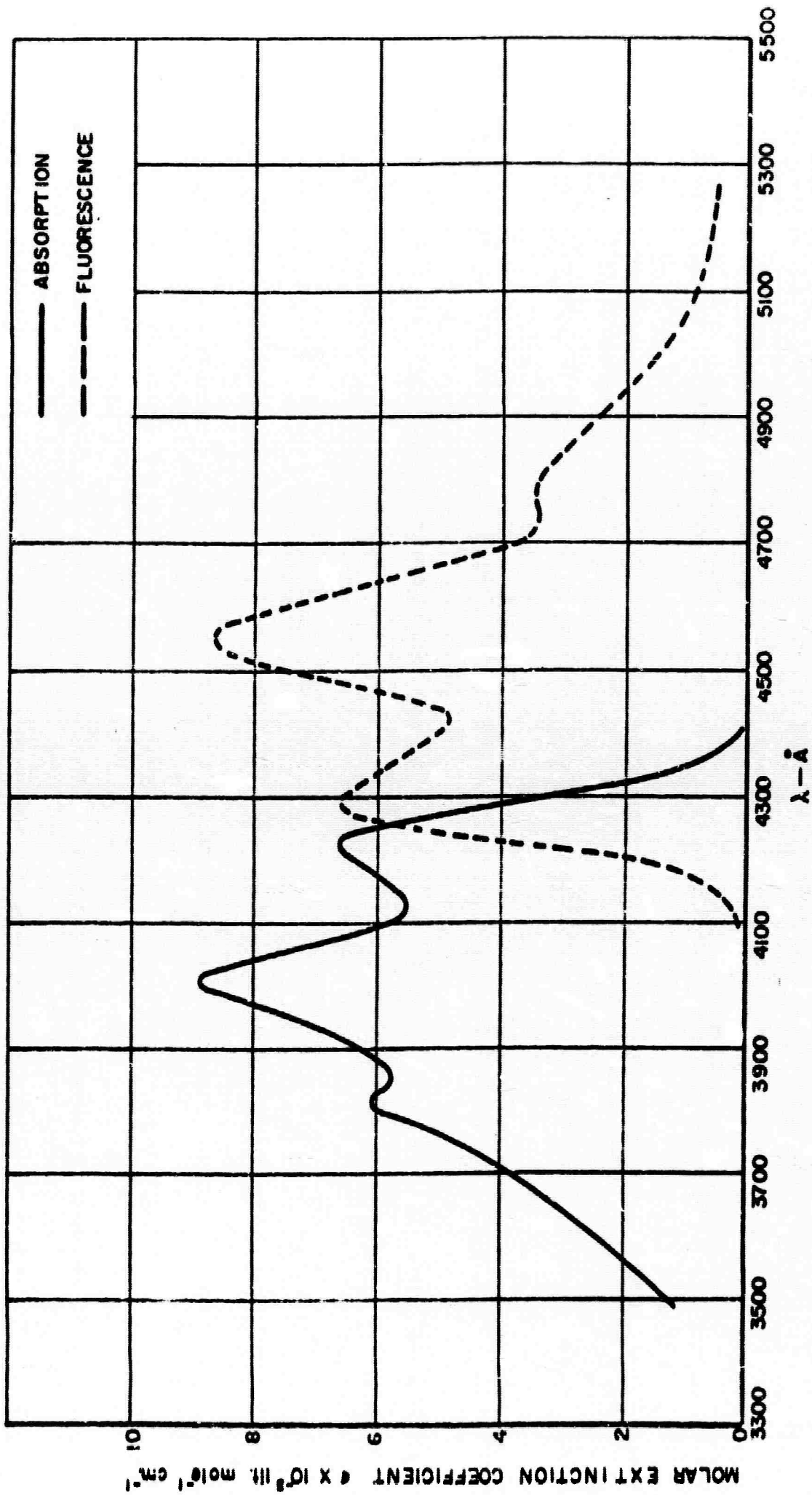
2. 9-Aminoacridine

9-Aminoacridine exhibits a very high fluorescence efficiency in a wide variety of solvents⁽¹⁹⁾. Table 1 shows the measured quantities for this molecule in various solvent systems. The absorption and fluorescence spectrum of 9-aminoacridine in water is shown in Figure 6. Water was chosen over ethyl alcohol-HCl as a host since the life time is longer at comparable quantum efficiencies and because the potential stimulated emission band at 4540 Å is higher than the side bands whereas in ethyl alcohol-HCl, this effect is not so pronounced.



LONG WAVELENGTH ABSORPTION OF 5.56×10^{-4} MOLAR PERYLENE IN BENZENE (10cm PATH LENGTH)

FIGURE 5



ABSORPTION AND FLUORESCENCE SPECTRUM OF 9-AMINOACRIDINE IN H₂O.
 FIGURE 6

TABLE 1

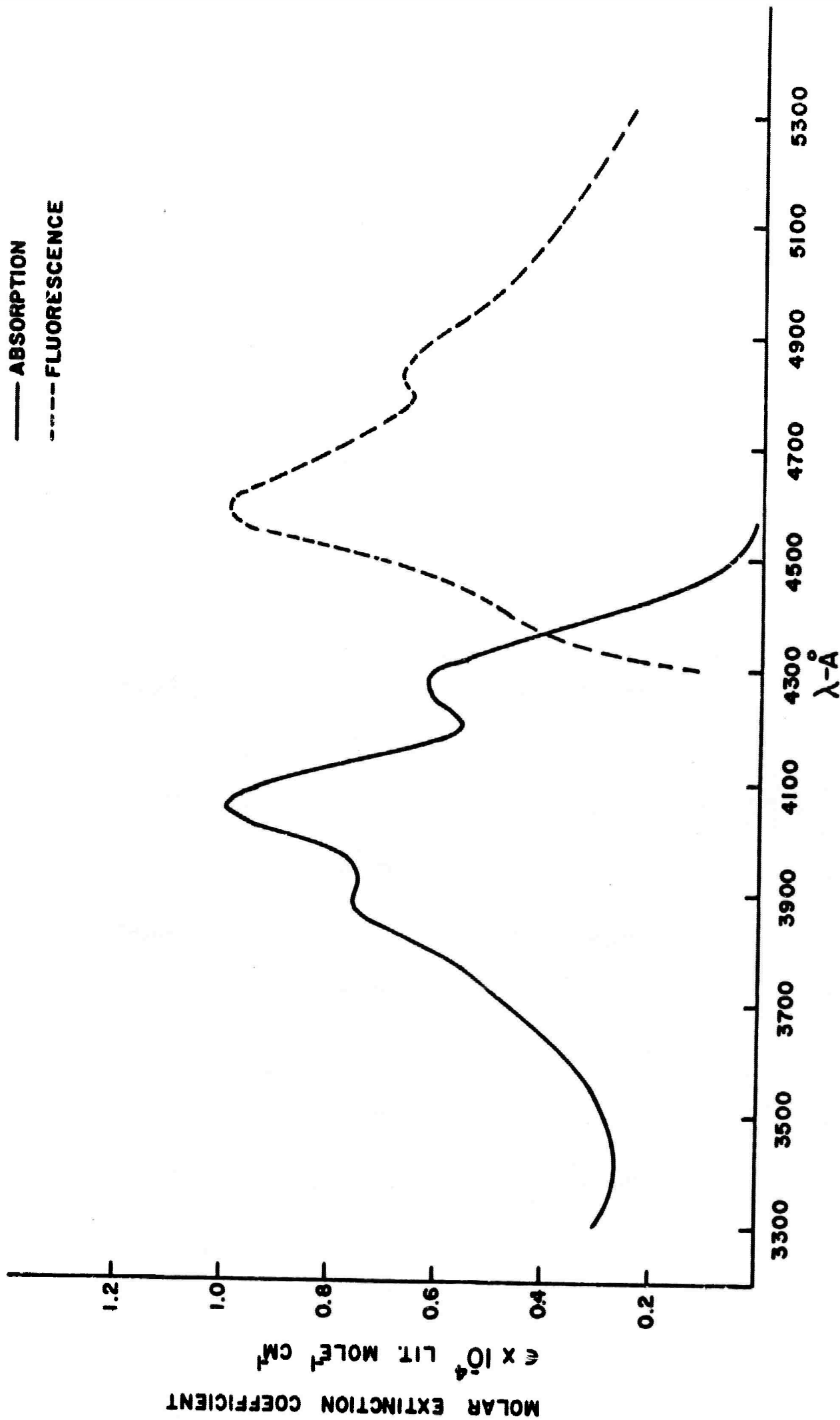
Lifetimes and Quantum Efficiency - 9-Aminoacridine
(after Strickler and Berg⁽¹⁹⁾);

Solvent	$\tau \times 10^9$	$\tau_0 \times 10^9$	ϕ
Ethyl Alcohol	13.87	15.43	0.899
Ethyl Alcohol HCl	14.07	14.19	0.994
Water	16.04	16.40	0.978
Water-HCl	15.45	16.67	0.927

The absorption and fluorescence spectrum in the modified polymethyl methacrylate host measured on a sample whose concentration was 1.5×10^{-4} moles per liter is shown in Figure 7 (where the highest energy fluorescence band has undergone partial reabsorption). The terminal-ground state separation is 1350 cm^{-1} . The four-level fluorescence band peak is located at $4582 \text{ \AA} \pm 1 \text{ \AA}$.

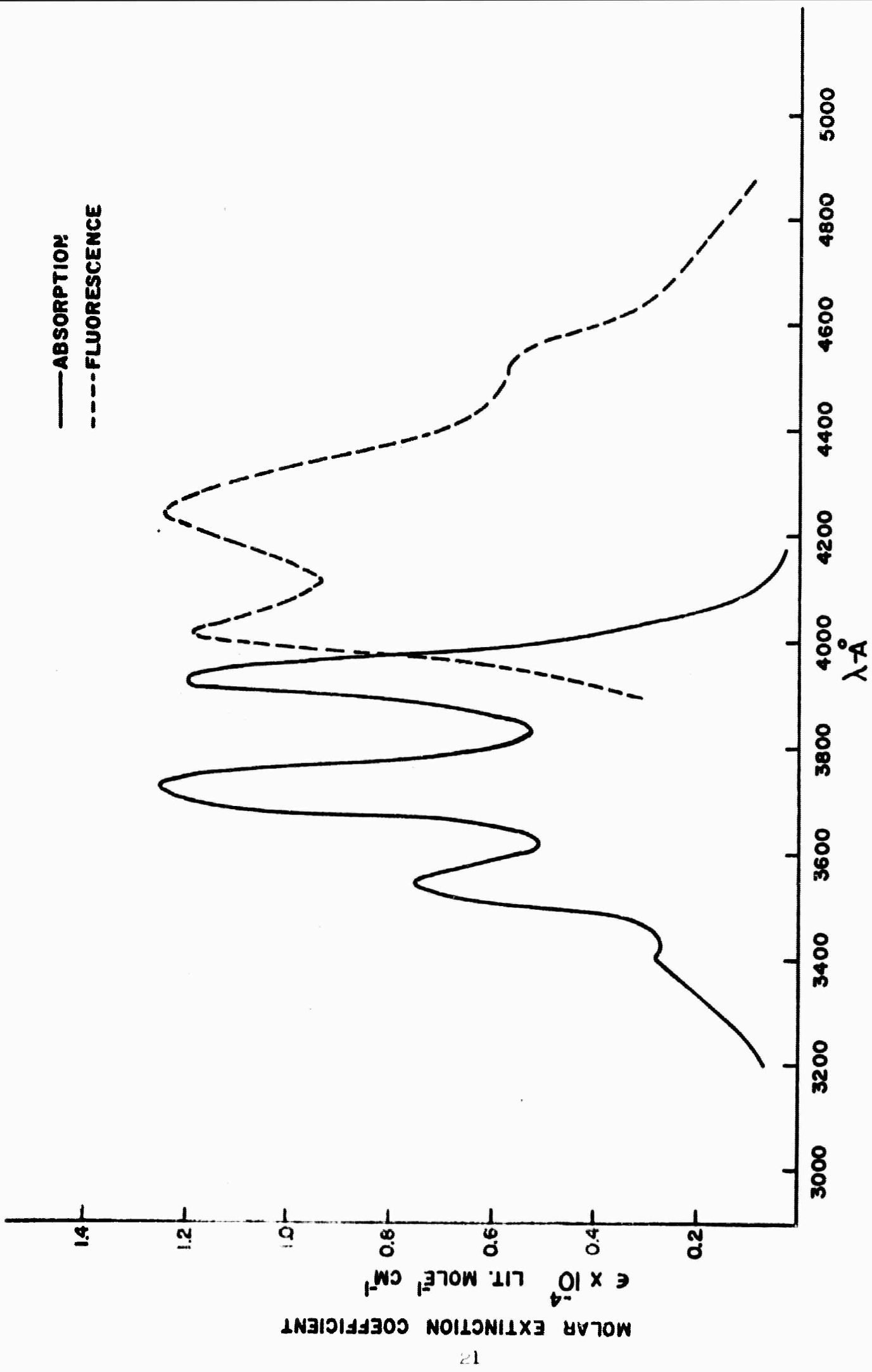
3. 9,10-Diphenylanthracene

The absorption and fluorescence of 9,10-diphenylanthracene in isooctane is shown in Figure 8 and its characteristics in the polymer in Figure 9. The measured terminal-ground state splitting is about 1600 cm^{-1} . In the polymer the four-level fluorescence peak is located at $4266.5 \pm 1 \text{ \AA}$. The fluorescence lifetime and quantum yield measurements given by Bowen⁽²¹⁾, Ware and Baldwin⁽²²⁾ and Birks and Dyson⁽²³⁾ are in good agreement. In benzene, $\tau_0 = 7.9 \times 10^{-9}$ sec, $\tau = 7.3 \pm 1 \times 10^{-9}$ seconds and, therefore $\phi = 0.84$. In the polymer, is approximately the same while the relative quantum yield is higher. The quantum yield of this compound is sensitive to solvent viscosity since the principal mechanism of deactivation other than fluorescence

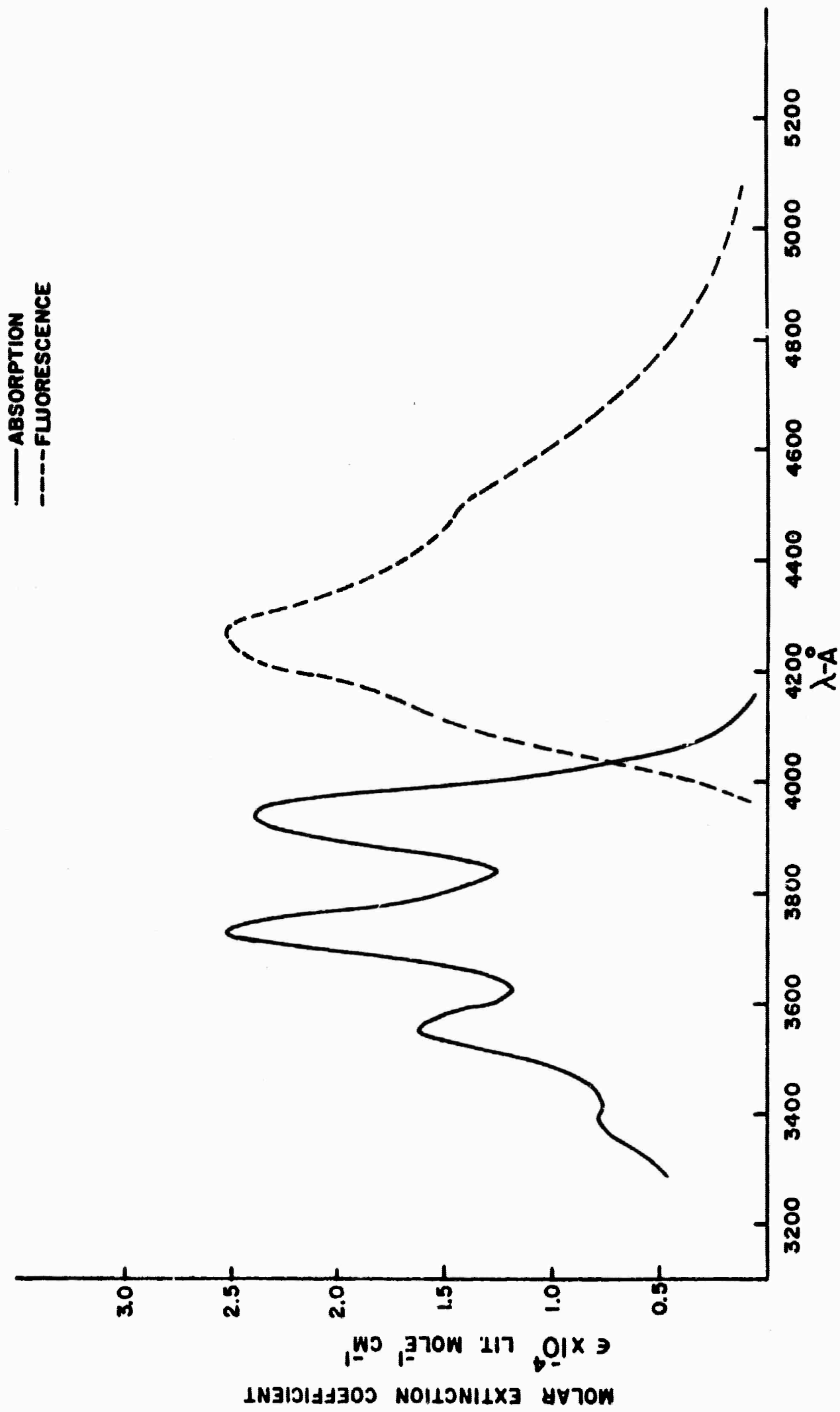


ABSORPTION AND FLUORESCENCE OF 9-AMINOACRIDINE IN PMMA-10.5% DBP

FIGURE 7



ABSORPTION AND FLUORESCENCE SPECTRUM OF 9,10-DIPHENYLANTHRACENE IN ISOCTANE
 FIGURE 8



ABSORPTION AND FLUORESCENCE SPECTRUM OF 9,10-DIPHENYLANTHRACENE IN PMMA-10.5% DBP

FIGURE 9

is quenching at a diffusion-limited rate by ground state molecules. In the polymer, therefore, the quantum efficiency is virtually unity as measured by the relative intensity of two samples of the same geometry, refractive index and concentration.

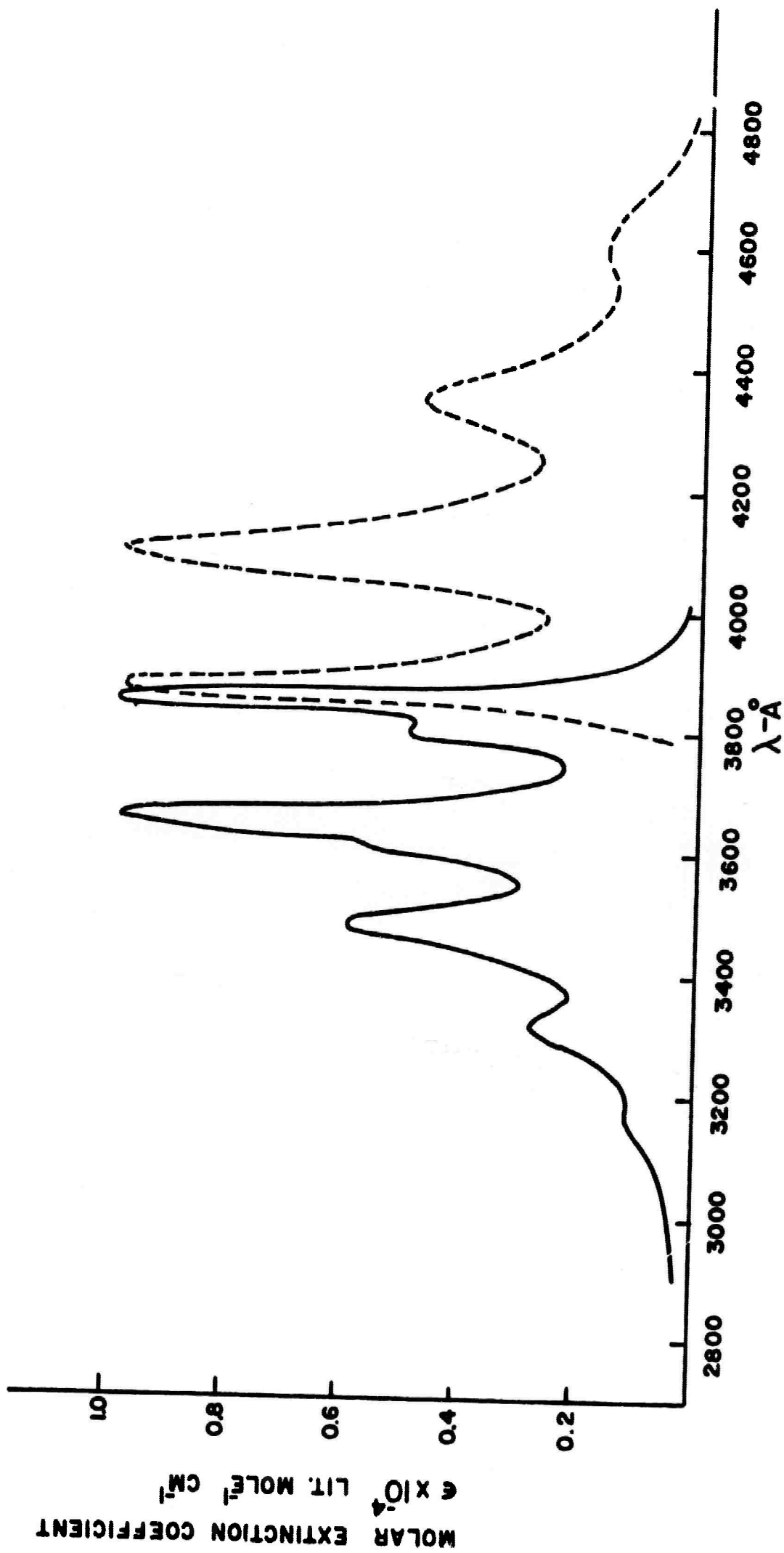
4. 9-Methylanthracene

The absorption and fluorescence of 9-methylanthracene in hexane is shown in Figure 10 and in the polymer in Figure 11. In the polymer, the fluorescence peak is at $4137 \text{ \AA} \pm 1 \text{ \AA}$ with a terminal-ground state separation of 1500 cm^{-1} . The only quantum efficiency measurements in the literature are those made by Bowen and Sahu⁽²⁴⁾ who found a very large viscosity effect for the quantum yield of fluorescence. They report quantum efficiencies of ~ 0.6 in toluene at room temperature increasing to ~ 1.0 at -50°C . In a polymer, the quantum yield should be virtually unity at room temperature. The intrinsic lifetime calculated from the absorption spectrum (in hexane) is $13-15 \times 10^{-9}$ seconds.

5. Rubrene

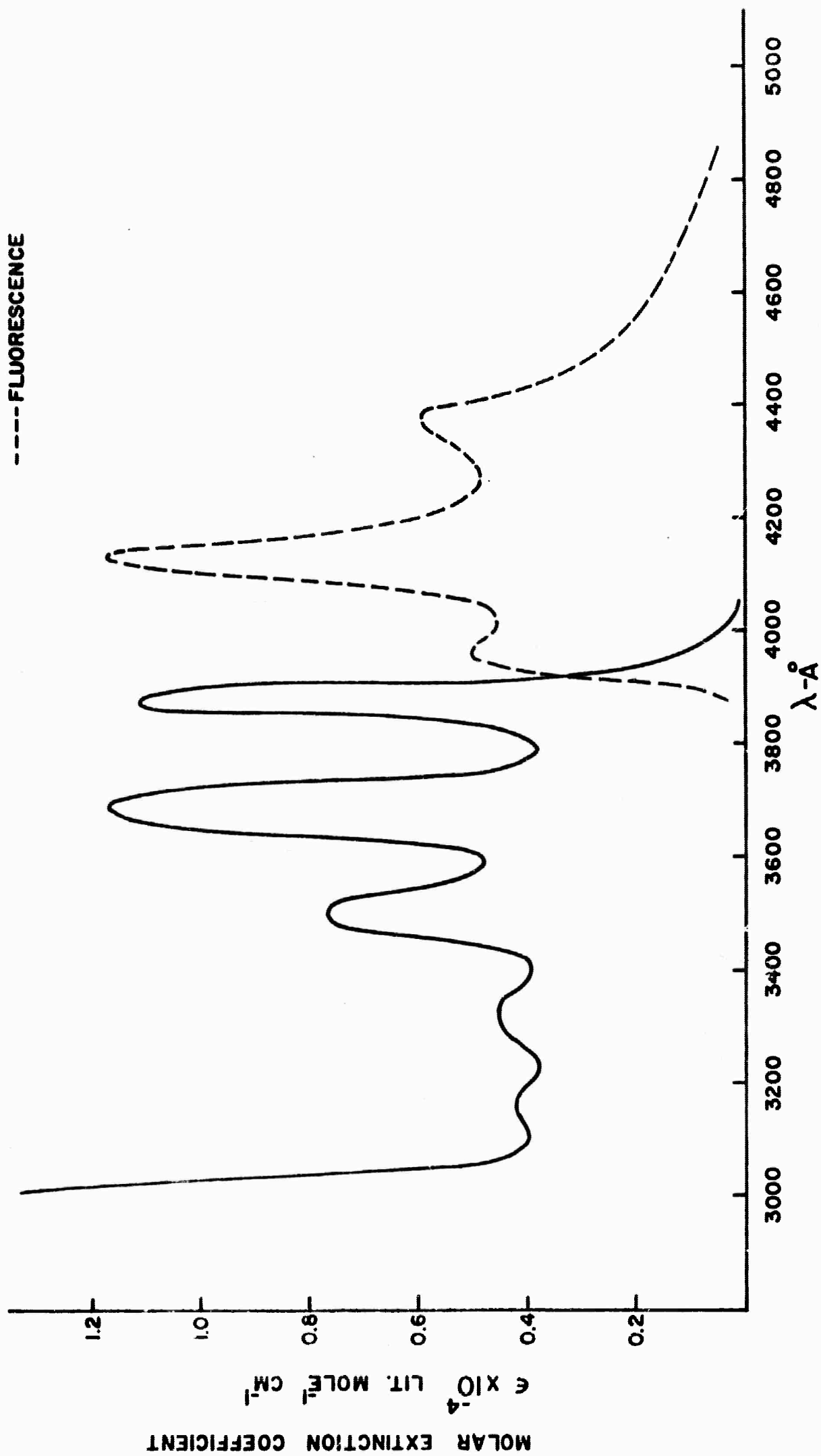
Rubrene (9,10,11,12-tetraphenylnaphthacene) is a molecule which exhibits four-level characteristics. The absorption and fluorescence in solution and in the polymer is shown in Figures 12 and 13. Although the quantum efficiency is only 0.73 in benzene⁽¹⁹⁾ and is photochemically unstable, it was felt that incorporation within the polymer would significantly increase the quantum yield and hence lower the rate of photodegradation. The quantum yield did increase markedly in the polymer, but under high flash intensities, rubrene still proved to be photochemically unstable.

— ABSORPTION
- - - FLUORESCENCE



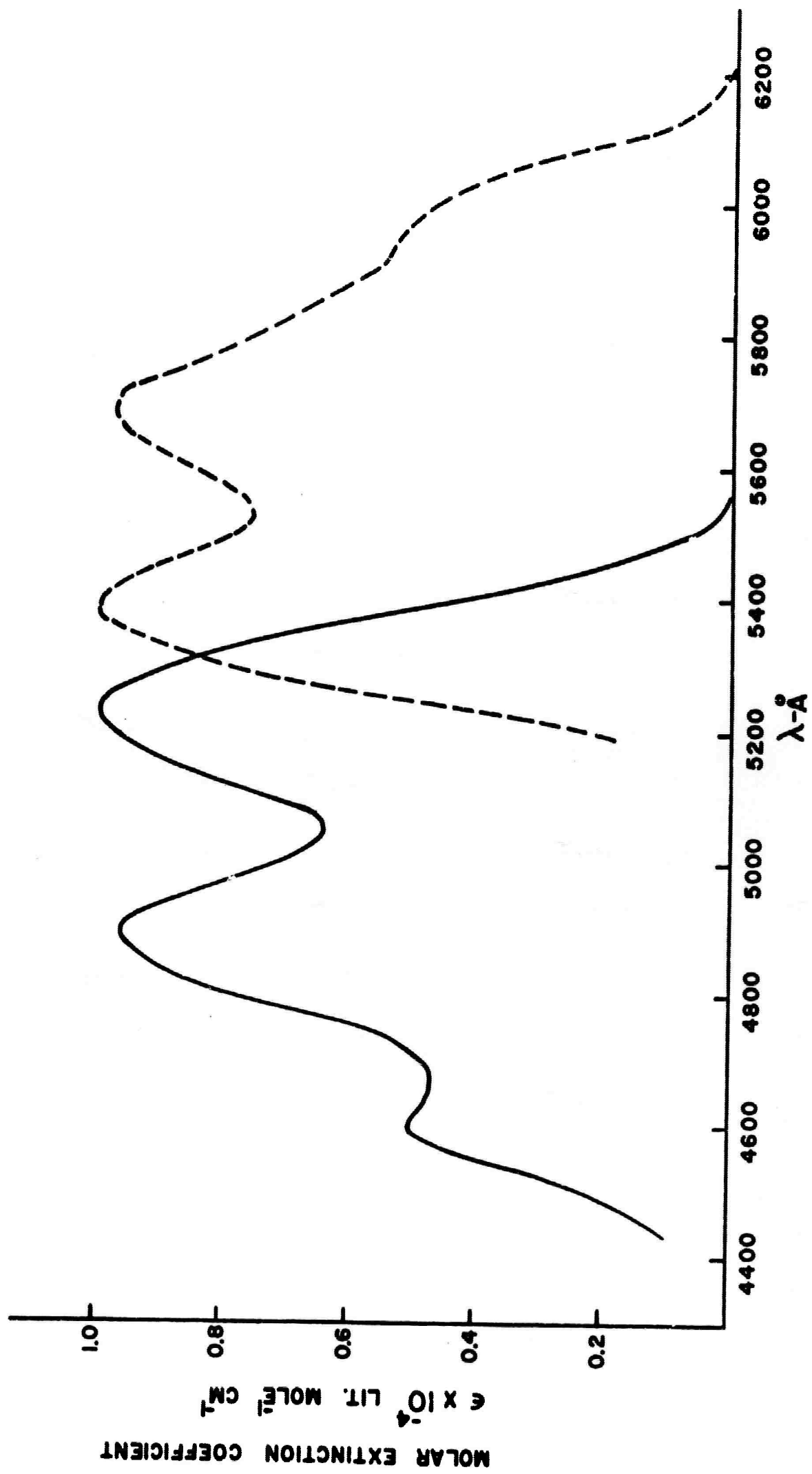
ABSORPTION AND FLUORESCENCE OF 9-METHYLANTHRACENE IN HEXANE
FIGURE 10

— ABSORPTION
- - - FLUORESCENCE



ABSORPTION AND FLUORESCENCE OF 9-METHYLANTHRACENE IN PMMA-10.5% DBP

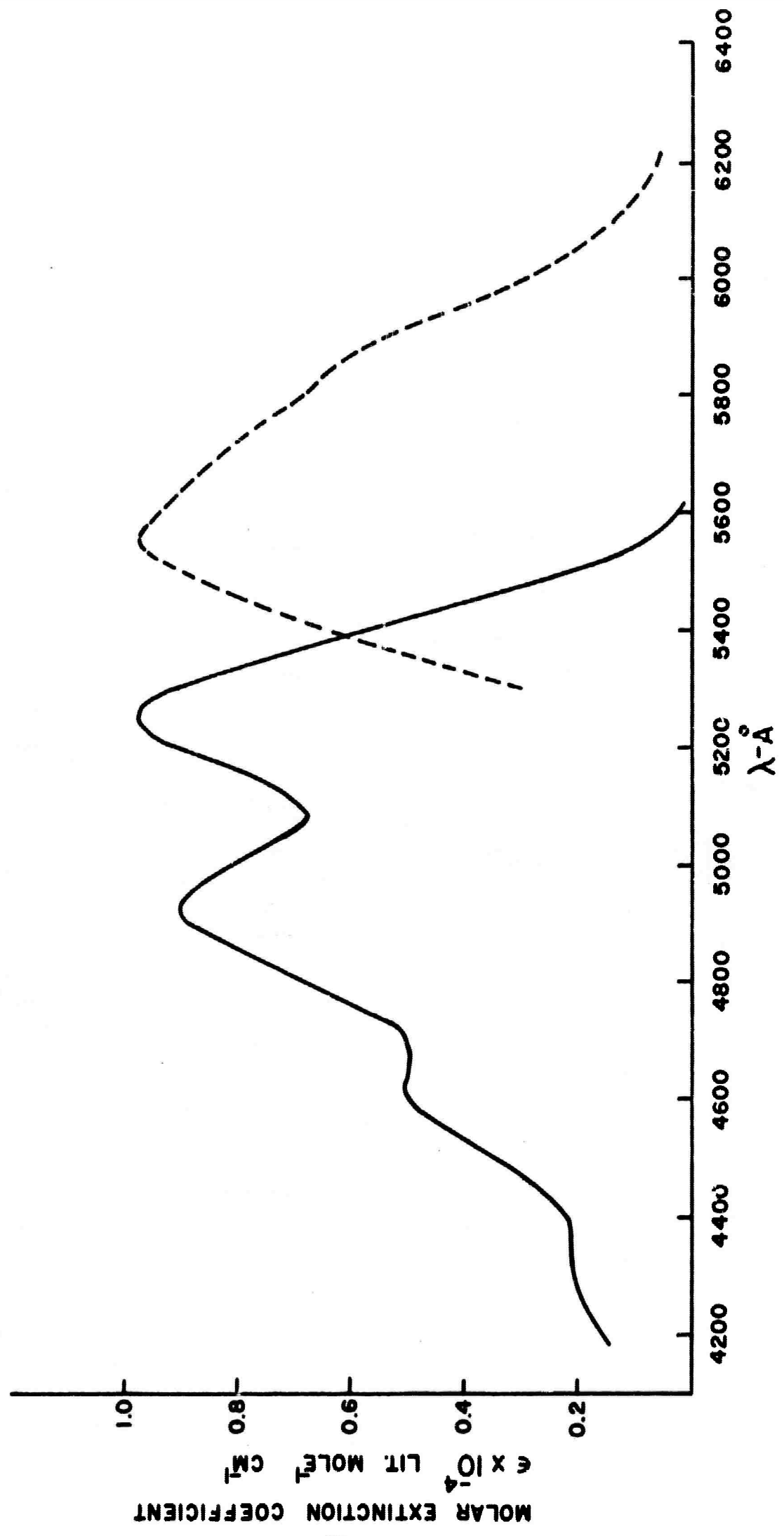
FIGURE II



ABSORPTION AND FLUORESCENCE OF RUBRENE IN HEXANE

FIGURE 12

— ABSORPTION
- - - FLUORESCENCE



ABSORPTION AND FLUORESCENCE OF RUBRENE IN PMMA - 10.5% DBP

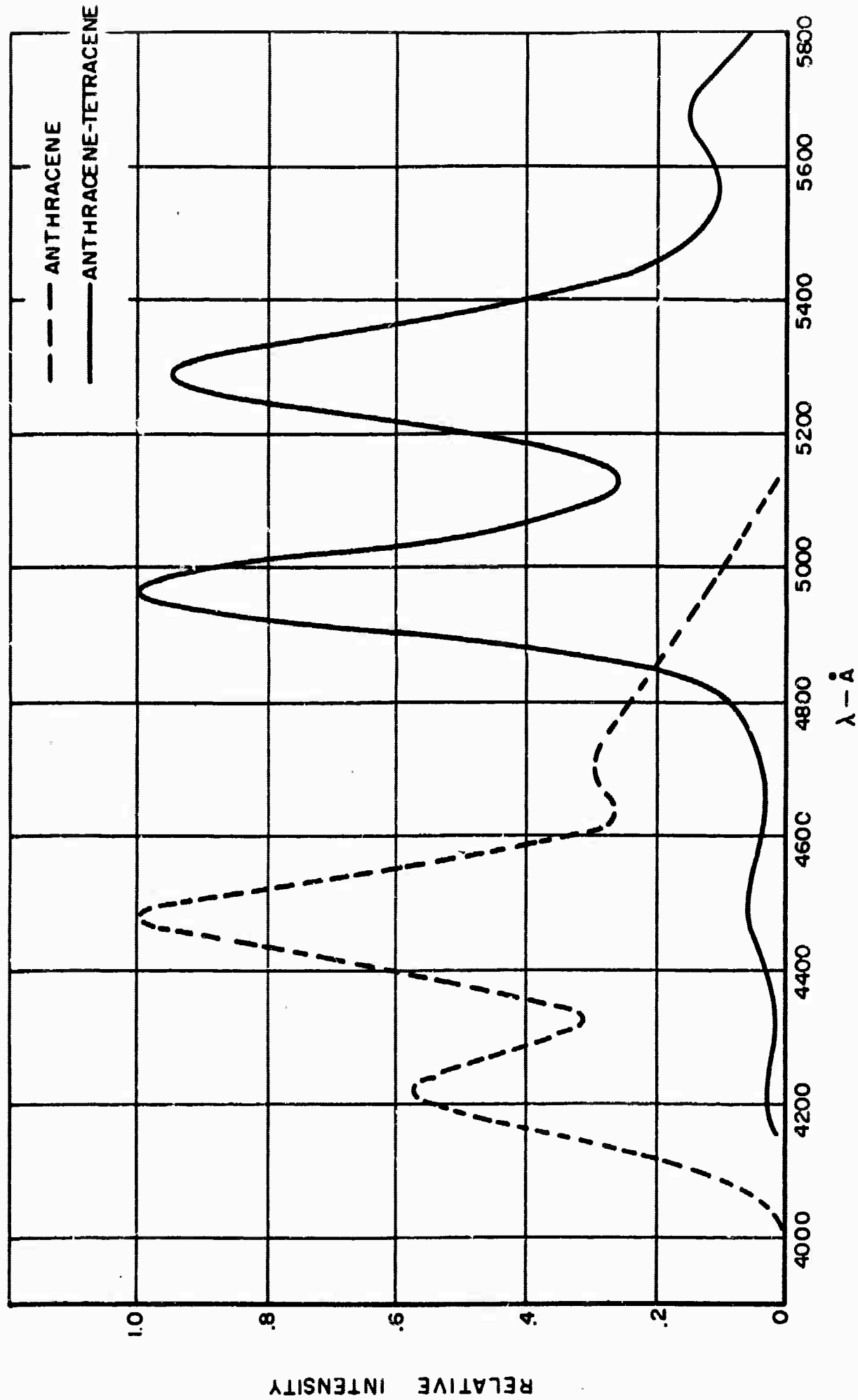
FIGURE 13

6. Naphthacene in an Anthracene Crystal

The last system studied which showed good potential organic laser material is the molecule naphthacene (tetracene) in an anthracene single crystal. This mixed crystal system represents a rather different type of potential organic laser material. Anthracene as a pure crystal is fluorescent with a quantum efficiency of at least 0.9 and possibly 1. The fluorescence lifetime is 18.8×10^{-9} seconds⁽²⁵⁾. It has absorption and fluorescence bands very similar to the perylene molecule with the fluorescence spectrum at room temperature being shown in Figure 14. One feature of the fluorescence of anthracene is the very rapid rate at which the excitation energy migrates through the crystal before emission occurs⁽²⁵⁾.

Upon addition of the naphthacene molecule in concentrations of the order of 10^{-4} molar (6×10^{16} molecules/cm³), the radiation absorbed by the anthracene is transferred with unit efficiency to the naphthacene molecule where it fluoresces. The fluorescence spectrum of a mixed crystal of naphthacene and anthracene at room temperature is also shown in Figure 14. The anthracene fluorescence is almost completely suppressed by the emission of the naphthacene. In these experiments the naphthacene was not directly excited in order to obtain the spectrum shown in Figure 14. The diffusion of the excitation energy into the crystal must occur much more rapidly than the lifetime of the excited singlet states. This system could be pumped optically in two ways.

1. The normal pump power penetration of the crystal corresponding to the region 4000-4700 Å absorption of naphthacene where the anthracene crystal is optically clear.
2. The absorption of light by the anthracene itself at the surface with virtually no penetration of the incident radiation, the energy then being transferred into the center of the crystal extremely rapidly. Calculations of the anticipated threshold for such a system show the same range of input powers as for the other systems discussed above since naphthacene is a four-level system with a terminal-ground state separation of about 1300 cm^{-1} .



FLUORESCENCE SPECTRUM OF SINGLE CRYSTAL ANTHRACENE AND SINGLE CRYSTAL ANTHRACENE -10⁻³m. TETRACENE.

FIGURE 14

Proper orientation of the crystal axes with respect to the resonant axis would be of some importance since the naphthacene fluorescence is polarized along the a and b molecular axes with the ratio $\frac{b}{a} = 1.9^{(26)}$. Other mixed crystal systems offer similar possibilities although all of the properties relevant to a potential laser material have not yet been investigated.

B. Preparation of the Liquid Samples

The liquid solutions were prepared by taking known quantities of the recrystallized compounds and dissolving them into the appropriate quantities of freshly chromatographed reagent-grade solvent. The concentration used was consistent with the best possible absorption of the radiation. The solutions were degassed on a vacuum line by alternately freezing, pumping and thawing exhaustively. The cell was then sealed off under high vacuum. This served to remove all traces of oxygen which exhibit deleterious effects of the excited states of these molecules. Samples prepared in this manner were stable for several hundred flashes under the conditions of low energy (less than 300 joules) and high peak power.

The liquid cell is constructed of thick walled pyrex tubing 6 centimeters long and about 0.6 centimeters in diameter. The end windows are of optically flat quartz and are bonded to the pyrex tube with a special epoxy resin after the pyrex tube is machined to insure reasonable parallelism of the windows. Exact parallelism of the windows is not critical since the optical alignment of the Fabry-Perot or confocal cavity is made through the sample and thus any small wedge effects are taken into account.

C. Selection of Plastic Hosts and Their Preparation

There are many plastic materials available which potentially could act as a host for an organic dye in a resonant cavity. However,

most must be discarded because of a lack of optical clarity, a significant absorption in the blue region of the spectra or a lack of dimensional stability and hardness. The Polyolefins, Polyamides, Epoxies and Polyesters, Polyacetals, Polyvinyls and all modified Polystyrenes are not satisfactory in this respect. A few of the relevant properties of the remaining materials are listed in the table below.

	Impact Strength D-256 ft lb/in. of notch	Rockwell hardness D-785	Heat Dis- tortion D-648	Water Absorb- tion 24 Hours D-570	Light Trans- mission 4000- 7000 A	Re- fractive Index
Polycarbonate	14	R116 (M-78)	270°F	0.35%	86%	1.586
Polystyrene	0.45	M-72	185°F	0.04%	89%	1.590
Cellulose Acetate	6	R52	123°F	2.4 %	90%	1.480
Cellulose Acetate Butyrate	7	R61	135°F	1.4 %	90%	1.475
Methyl Methacrylate	0.4	M-97	198°F	0.3 %	93%	1.490

The data above are given according to the noted ASTM specification. The transmission data do not take into account the Fresnel reflection. Thus, the 93% for methyl methacrylate should be 99+%.

The cellulosic materials were eliminated because of the lack of dimensional stability as well as the low hardness value. The hardness value is an indication of the degree to which a material may be polished and continue to maintain acceptable surface characteristics. Neither of the cellulose materials meet these requirements.

After examining some polystyrene rod, and molding some pure pellets, styrene monomer was obtained and polymerized in the absence of catalyst to give

a particle free styrene blank of extremely fine apparent optical quality. Machining characteristics and subsequent dimensional stability were observed for polystyrene. In passing plane polarized light through a polystyrene rod, it was found to be depolarized. It is possible that the styrene molecule causes this effect or that the cast and machined rod was very highly oriented. This effect was not related to normal strain effects. In addition, oxygen diffusion in polystyrene is very rapid which will affect the excited states of the fluorescent compounds.

The desire to investigate a polycarbonate comes from the properties of higher heat resistance and greater impact strength. However, the best available polycarbonates exhibit scattering to a large extent and are, therefore, unsatisfactory. They cannot be prepared by in situ polymerization as they require a catalyst bed.

Polymethyl methacrylate was then investigated. This material has even greater hardness than polystyrene and in fact, machines as well or better. In addition, oxygen diffusion into the material is very low.

There are several potential methods of preparing polymeric methyl methacrylate. They are: (1) Thermally grown polymer from the monomer without the use of a catalyst, (2) Extrusion, (3) Injection molding, (4) Compression molding, (5) In situ polymerization. Four of these five techniques were attempted in the program.

1. Thermal Polymerization

The thermal polymerization was initiated at about 85°C in a teflon-lined, evacuated glass tube containing the unstabilized monomer and the desired concentration of perylene. After several days at this temperature the polymerization was complete. The samples were quite hard and could be easily machined and polished. However, due to extensive cross-linking of the polymer, the molecular weight was so high that the samples exhibited no softening point without depolymerization and thus could not be annealed to remove density gradients.

2. Extrusion

Extrusion was the next technique attempted. The molecular weight of the thermally polymerized material was too high to be used as an extruding material since it thermally depolymerized at the temperatures necessary for extrusion. It was found possible to extrude an "optical grade" Rohm and Haas plexiglass molding powder called V-100. This material was extruded with both the perylene and 9-aminoacridine dyes in the form of a 1/4" diameter rod. The 1/4" rods exhibited a radially directed strain. Annealing in air and in mineral oil was attempted at various temperatures for several days followed by slow cooling but the density gradient could not be removed completely.

3. Compression Molding

The third technique attempted was to compression mold the material followed by careful annealing in the mold. Sample rods formed in the mold were 0.260" in diameter and 3" long. An extruded rod was used as the starting material and the rod was incorporated into the mold and heated to the desired temperature (a range of 100-200°C was employed) where it was allowed to soak for a period of time varying up to two hours. Pressure was then applied in stages to the final desired pressure which ranged from 1,000 to 10,000 psi. The samples were then cooled slowly over a period varying from 4 to 48 hours. The optimum molding conditions were found to be 135°C and 2750 psi with a soak cycle of one hour and a cooling time of at least 12 hours. The samples made in this way exhibit smaller gradients than samples prepared by other techniques used to date. There was a residual strain at the end of the rods where the pressure had been applied and a minor amount of strain where the rods were in contact with the split in the mold. It was found possible to remove the strains by careful annealing in mineral oil at a temperature of 100 to 105°C followed by slow cooling. Such samples exhibited no detectable strain for 3-4 days after the annealing was completed. Subsequently, the end strain reappeared, however. It has not proved possible to date to reanneal the end strain out of the compression molded rods on a permanent basis.

It was deemed of some importance to investigate the light scattering properties of a good compression molded rod as compared to the best optical grade plastics available. These measurements of the scattering show that the compression molded rod scattered light by a factor of 30 more than was the case for a (undoped) rod prepared by commercial casting techniques, indicating that the optical grade V-100 plexiglass used in the compression molding studies is really inferior in this respect. An absolute figure for the scattering by the compression molding rod is difficult to assess but it is in the range of 0.01 to 0.03 per cm. On this basis the scattering of the rods prepared by the casting techniques must be about 0.001 per cm.

4. In Situ Polymerization

The process to be described in this section proved to be the one that was most satisfactory. During the early studies described above, the effects of the molecular orientation of the polymer on the birefringence were not understood completely, but evolved gradually as the program went along. Samples were prepared by in situ polymerization and exhibited good optical properties except for the fact that they exhibited stress-birefringence.

Stress-birefringence in polymers arises because of steric hinderance of the chemical groups within the polymer chain. Two states of the polymer exist which differ in their elastic characteristics. The "glassy" state, present at room temperature in most polymers, is characterized by a polymer structure so tight and rigid that only short range distortion, i.e., steric hinderance, is observed. In the "rubbery" state, the molecular chains can uncoil and extend and thus distortions are propagated over large distances. Andrews and Rudd⁽²⁷⁾, Stein⁽²⁸⁾ and Gurnee⁽²⁹⁾ have discussed these effects in detail. The transition between these two states is, thermodynamically, second order. For polymethyl methacrylate (PMMA), the transition temperature is near 40°C⁽³⁰⁾. When the polymer is annealed, the cooling cycle must pass through this temperature. Since exact

thermal equilibrium cannot be maintained during this transition, the internal stresses are still observed and the samples are birefringent. One way to obviate this problem is to design the polymer so that it possesses a zero stress-optical coefficient.

The birefringence Δn , introduced into a sample as a result of the application of a pressure per unit area F' , is given by

$$\Delta n = KF'$$

where K is the stress-optical coefficient.

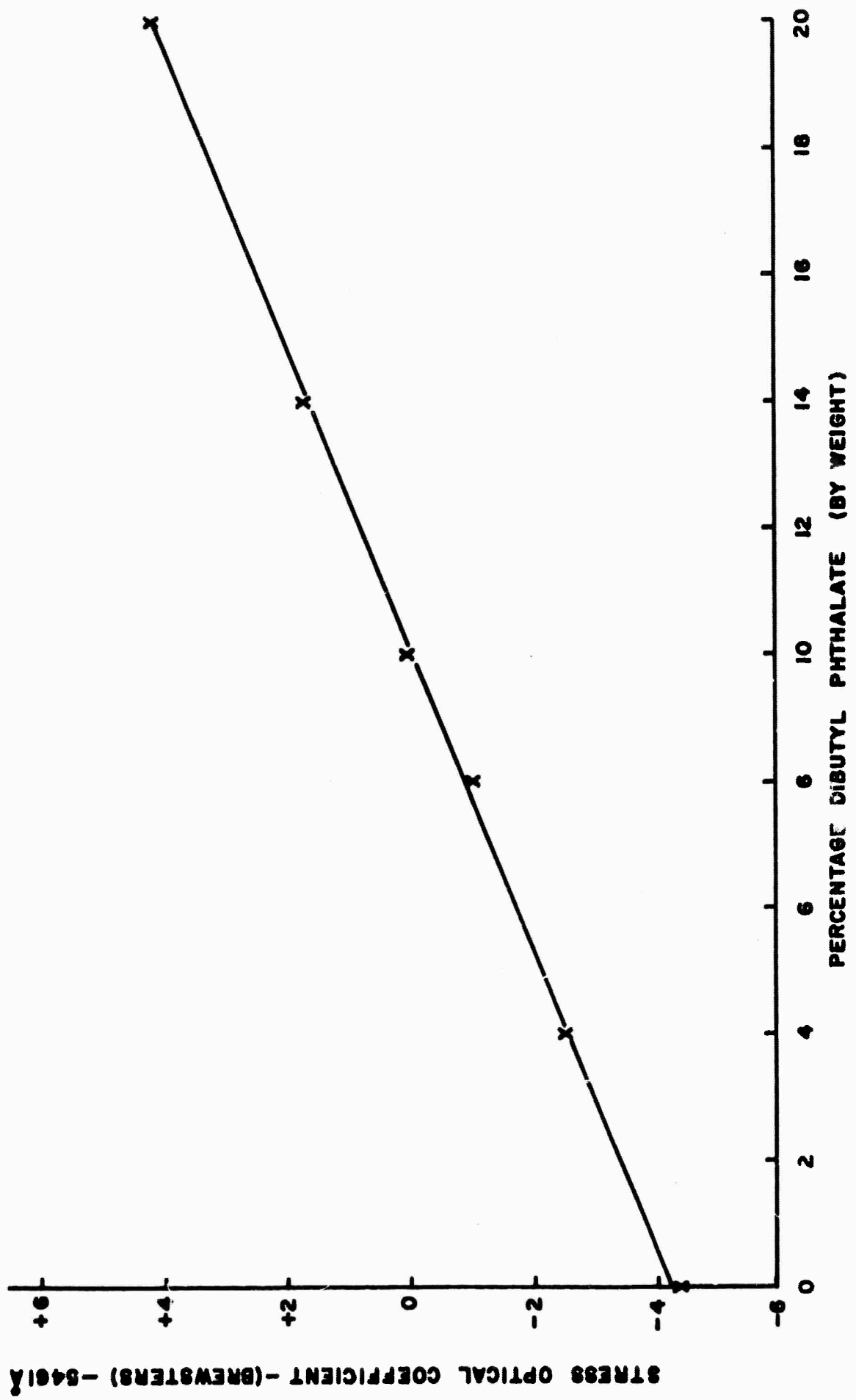
Pockels in his early studies⁽³¹⁾ on glasses had developed a glass exhibiting a zero stress-optical coefficient. More recently, Lambie and Dahmouch⁽³²⁾ had shown that this is possible in a polymer by the addition of dibutyl phthalate (DBP) to the methyl methacrylate monomer. Their studies showed that varying amounts of DBP added to the methyl methacrylate monomer produced a polymer with a stress-optical coefficient which varied from about -4 Brewsters for the pure polymer to $+4$ Brewsters for the 20% by weight-doped polymer.* A principal difficulty with their study was the large stresses employed on thin samples (to give measurable retardations), giving rise to some irreversible effects. Also, for our purposes, the values given were not accurate enough.

We repeated this work since our polymerization technique involved a different catalyst and a different curing cycle. Measurements on the stress-optical coefficient as a function of composition were made using a collimated mercury source used at 5461 \AA in conjunction

*For our purposes, we have adopted the convention employed by others⁽³²⁾ that a compressive stress in PMMA corresponds to a negative stress-optical coefficient.

with Glan-Thompson prisms and a quarter wave plate whose retardation error was $\pm 50 \text{ \AA}$. The minimum was determined visually and photometrically with no significant difference being observed. The samples were $0.6 \text{ cm} \times 0.6 \text{ cm} \times 7.5 \text{ cm}$. Pressure was applied using a hydraulic press on the $0.6 \times 7.5 \text{ cm}$ area in the range of up to 10^7 dynes per cm^2 in order to prevent the irreversible stressing of the material found by Lamble and Dahmouch⁽³²⁾. The retardation could be measured to $\pm 2^\circ$, resulting in a lower detection limit of the stress-optical coefficient of ± 0.05 Brewsters ($1 \text{ Brewster} = 1 \times 10^{-13} \text{ cm}^2 \text{ dyne}^{-1}$). In practice, although the retardations could be measured to $\pm 2^\circ$, the pressure applied was not uniform enough to permit accurate determination of the stress-optical coefficient to better than ± 3 Brewsters. The results are shown in Figure 15. They are essentially in agreement with the Lamble and Dahmouch results and it is evident from these data that approximately 10% by weight DBP is the composition required for a zero stress-optical coefficient material. Attempts to measure samples near the correct composition of 10% DBP were vitiated because of the small retardations encountered, in conjunction with the upper pressure limit available to us and the lack of uniform pressure over the path length. A series of samples were prepared ranging from 9-11% DBP in 0.1% intervals. After annealing at 110°C and polishing, the samples were examined under crossed Glan-Thompson polarizers. Samples containing 10.4 to 10.6% DBP were essentially free of birefringence with the 10.5% DBP sample exhibiting a birefringence, $\Delta n \leq 6 \times 10^{-7}$. These results were easily reproducible.

It was surprising to find that the 10.5% DBP sample did not exhibit a zero stress-optical coefficient. What has apparently happened is that the rubber-glass transition temperature (40°C in pure PMMA) has been shifted downward below room temperature for this composition. In order to test this hypothesis, we made measurements of the expansion of the polymer sample using a liquid dilatometer in the temperature range -20°C to $+45^\circ\text{C}$ in order to determine the glass-rubber transition temperature. The determination of the glass-rubber transition temperature was made



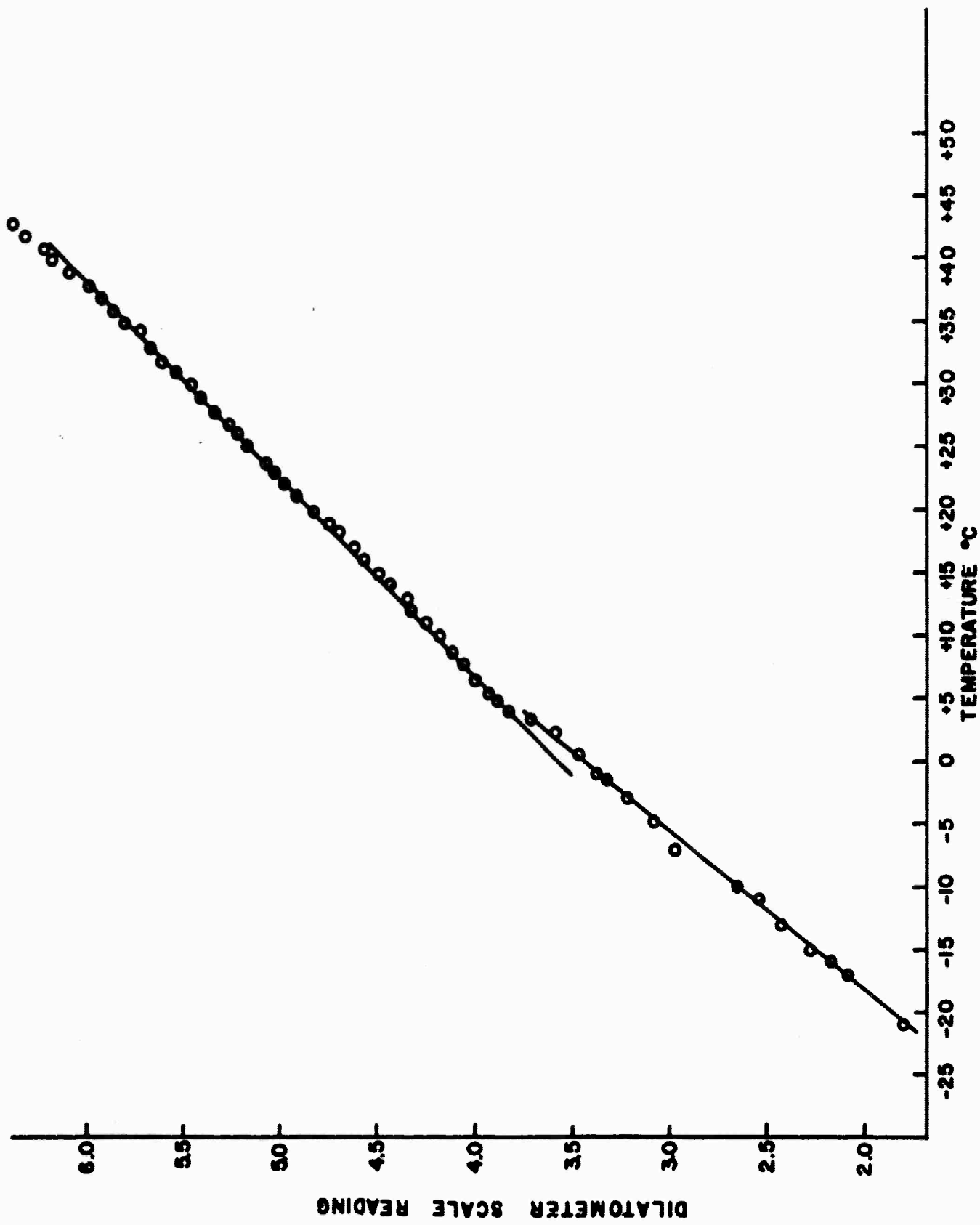
STRESS OPTICAL COEFFICIENT AS A FUNCTION OF DBP
FIGURE 15

using a liquid dilatometer which contained a polymer rod and was filled with a solution prepared by mixing 116 cc ethylene glycol and 84 cc water. Differential volume changes of 0.1% could be measured by this technique. The results are shown in Figure 16. It is evident that at about 5°C, the rate of expansion of the polymer undergoes a change and this would be expected for a (second order) transition from the (low temperature) glassy state to the (high temperature) rubbery state of the polymer. With the absence of the rubber-glass transition in the annealing temperature cycle, annealing to remove stresses is possible. This is consistent with the view that the transition temperature should decrease with the addition of DBP since the polymer chain is made more flexible and material stays rubbery at ever lower temperatures. The materials become birefringent again above this composition. Why the birefringence increases again above 10.5% DBP is not yet clear. Thus, the polymer developed is actually in a rubbery state.

The complete process for making an optically isotropic polymer can now be described. The methyl methacrylate monomer is treated to remove the stabilizing agent which consists of 25 ppm hydroquinone. The raw monomer is treated with a 20% NaCl, 5% NaOH water solution. Twenty cc of this solution is added for each 100 cc of the methyl methacrylate monomer. The mixture is shaken and placed in a separatory funnel. After separation, the material is dried for three hours over anhydrous NaCO_3 and then stored in a dry bottle under dry conditions.

The catalyst used is α, α' -azobisisobutyronitrile. It is used at a concentration of 0.03% by weight. The dibutyl phthalate was reagent grade and was used without further purification. These three components are mixed together and the necessary amount of fluorescent dye is added.

The pyrex tubes (1/2" ID) in which the polymerization would proceed are carefully cleaned. The solution is then put into the tubes via a syringe to which is attached a micropore filter. The particular filter system used as made by the Millipore Corp., Bedford, Massachusetts,



EXPANSION RATE OF 10.5% DBP - PMMA AS A FUNCTION OF TEMP.

FIGURE 16

and consists of two filters, one (AP2502200) to remove large gelatinous material and the second (NRWPO2500) to remove all dust particles present down to less than 1 micron in size. The cleaned tube is multiply-washed with the filtered solution before the actual filling operation. This filtering procedure makes a significant difference in scattering properties of the final rods. The filled tubes are then put on a vacuum line, the oxygen removed and the system backfilled with clean, dust-free nitrogen to about 1 atmosphere pressure. The tubes are then sealed off.

The tubes are then placed into a water bath and raised to 40°C. They are held there for two days. They are then slowly increased over a one-day period to 60°C and over another one-day period (in an oven) to 100°C. They are held at 100°C for three days and then cooled to room temperature.

The machining and annealing of the samples is an important part of their preparation. The rods are first annealed in a mineral oil bath at 110°C. This is accomplished by a proportional controller which raises the temperature to the annealing point at the rate of 10°C per hour. A three hour soak cycle at 110°C is provided and the samples are then brought back to room temperature at the rate of 2.0°C per hour. The rods are then carefully machined to about 0.5 mm oversize. They are annealed again to remove strains introduced by the machining operation. They are then taken to the final tolerances (being held in a collet) and then polished. The final lapping is done using an AB Metcloth 407158 cut cloth and 0.3 micron Linde-A alumina. During the lapping of the ends, the rods are surrounded by a polymer of the same toughness to permit good flatness to be obtained over the entire surface.

5. Optical Properties of the Polymer

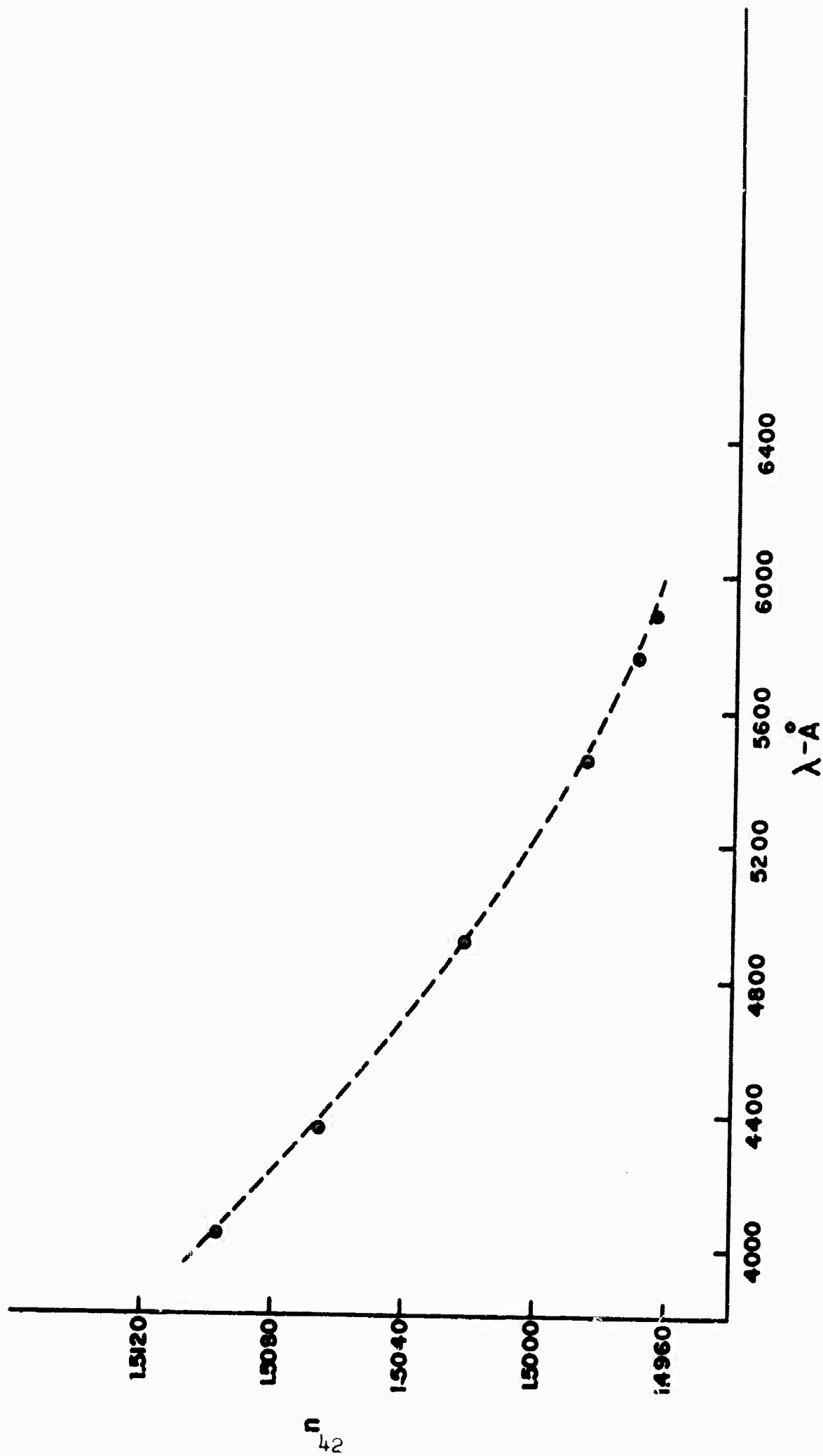
The refractive index and dispersion of the polymer were determined using minimum deviation angle measurements. The results are shown in

Figure 17. The dispersive power of the polymer is almost identical to that determined by other workers for normal methyl methacrylate polymers⁽³³⁾ and is comparable to other optical materials with this refractive index. Refractive index gradients within the sample were measured interferometrically. Qualitatively, gradients of the order of 5 parts in 10^5 were observed. This probably could be improved by further refinement of the annealing procedures.

Absorption measurements on a sample 1 mm thick were made with a Beckman DK-2 spectrophotometer and indicated that the sample is clear to wavelengths up to over 2 microns. The ultraviolet absorption is shown in Figure 18 where a constant Fresnel reflection correction has been made for the ultraviolet relative to the refractive index at 4046 Å. An optical density of 1 is observed at about 2575 Å. Between 2575 Å and 3,000 Å, the increase in apparent absorption observed could be due to anomalous dispersion and/or absorption.

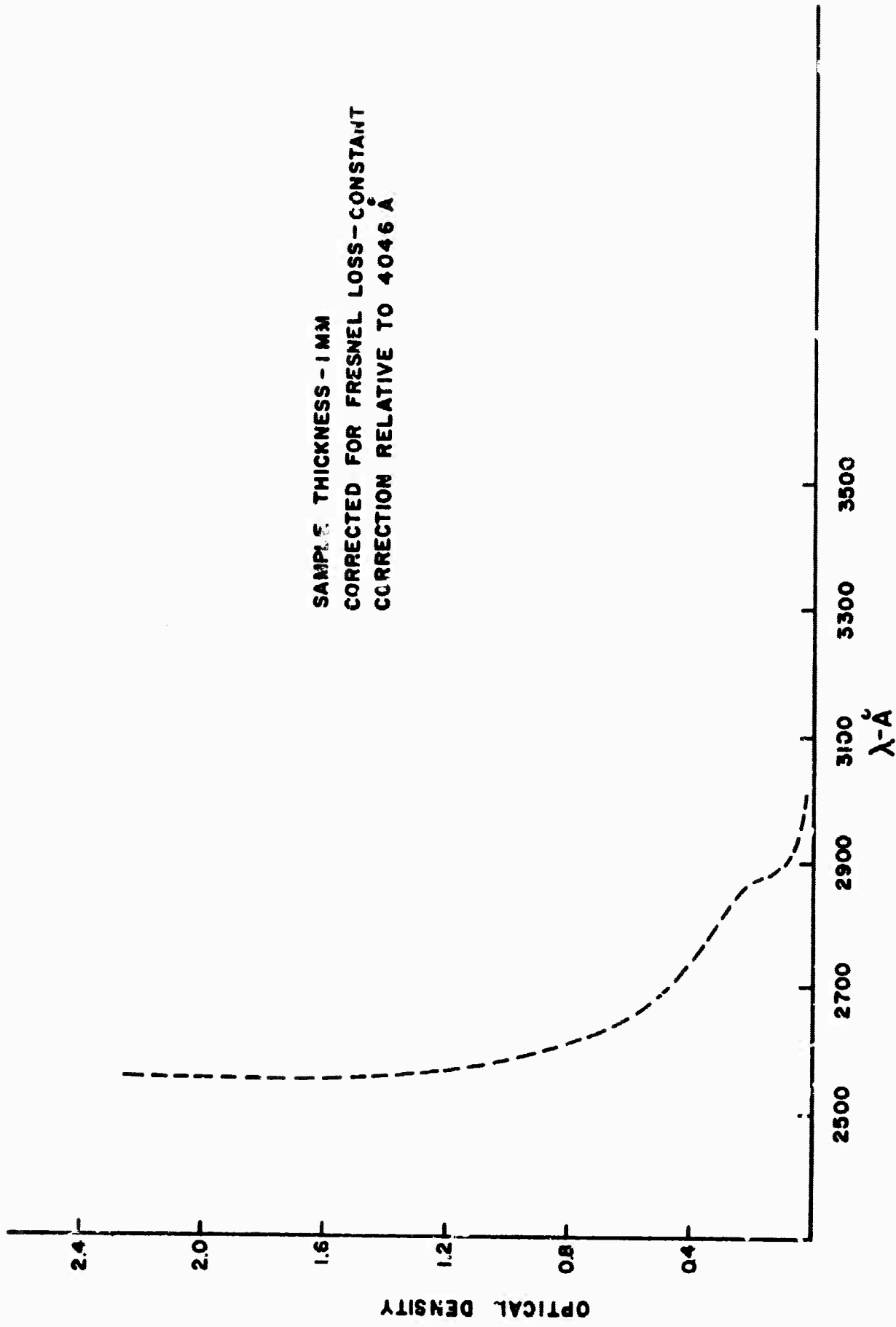
Expansion coefficient measurements were made using an NBS-designed expansion dilatometer manufactured by Industrial Instruments Inc., Allentown, Pa. This instrument is capable of measuring expansion coefficients two orders of magnitude smaller than encountered. Measurements were made only at increasing temperatures since the material depressed slightly under the spring loading.

Measurements were made of the expansion coefficient of the 10.5% DBP-PMMA material. The results are shown in Figure 19. The first portion of the curve at low temperatures is nonlinear due to lagging effects in the instrument but even the upper portion cannot be regarded as being linear. This may be due in part to the spring loading system of the instrument. However, a rough estimate of the expansion coefficient yields $\alpha = 3.2 \times 10^{-4}$ cm/cm°C. This is a slightly greater expansion coefficient than for commercially cast ("glassy") Plexiglas with $\alpha \sim 6 \times 10^{-5}$ cm/cm°C.



REFRACTIVE INDEX OF PMMA-10.5% DBP AS A FUNCTION OF WAVE LENGTH

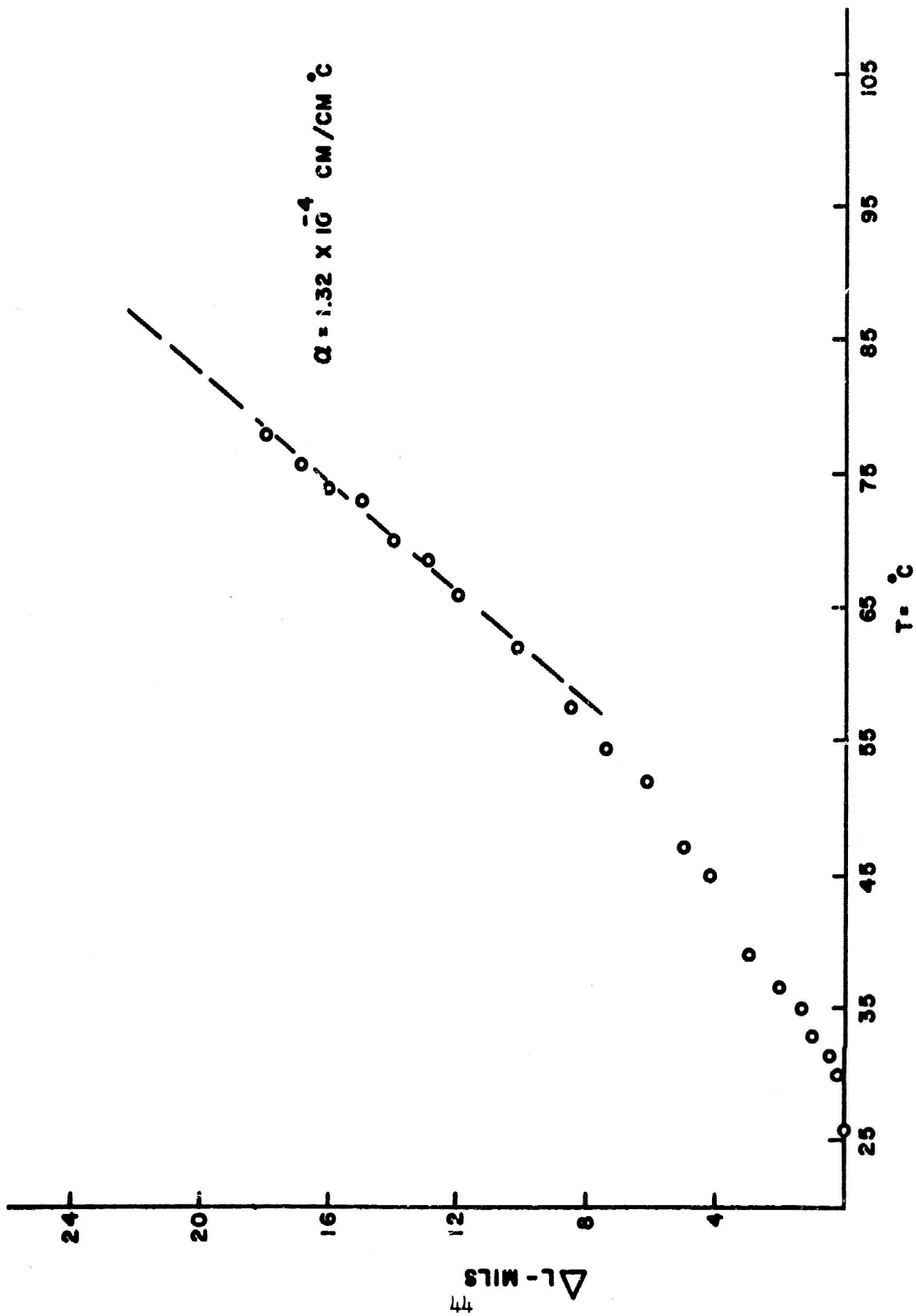
FIGURE 17



SAMPLE THICKNESS - 1 MM
 CORRECTED FOR FRESNEL LOSS - CONSTANT
 CORRECTION RELATIVE TO 4046 Å

ABSORPTION OF POLYMETHYL METHACRYLATE-10.5% DIBUTYL PHTHALATE

FIGURE 18



EXPANSION OF PMMA-10.5%DBP AS A FUNCTION OF TEMPERATURE

FIGURE 19

Measurements on the refractive index gradients within the sample were made using a helium-neon laser and a Michelson interferometer. A 5 mm diameter beam was used to insure large area observation. The fringe distortion was measured qualitatively on a sample 2.1 cm. long with optically flat ends. A photograph of the fringe system with and without the sample is shown in Figure 20. Also shown in Figure 20 is a picture taken under crossed Glan-Thompson prisms of the residual birefringence.

For these measurements, a cylinder of birefringent polymer closely surrounded the sample rod in the center. The sample rod was 10 cm long. The isogyre of the polymer cylinder can be seen. The small amount of center intensity in both pictures is due to off axis scattering into the center of the optical system from the polymer cylinder subsequent to the last polarizing unit.

Qualitatively, the hardness and dimensional stability of the samples are good after the annealing has been done. The samples can be polished, after the annealing procedure, to 1/10 wavelength flatness over areas in excess of 1 cm² and do not change in time. The polymer is particularly resistant to abrasion, can be cleaned with ordinary tissue and possesses good scratch resistance.

6. Characteristics of the Fluorescent Dye in the Polymer

One important question on the nature of the organic fluorescent dye concerns whether it is polymerized into the polymer chain or whether it is dissolved as an ordinary solute in the polymer. Although the doped polymer was extensively cross-linked, it proved to be slightly soluble in hot ethylene dichloride. Upon cooling the solution, a white polymer re-crystallized at the bottom and the fluorescent compound perylene remained in solution. This indicates that the dopant compounds do not enter into the polymer chains directly during the polymerization but are dissolved as an ordinary solute. Therefore, no polarization effects should be associated with the fluorescence of the molecule. Measurements failed to find any polarization associated with the fluorescence of perylene.

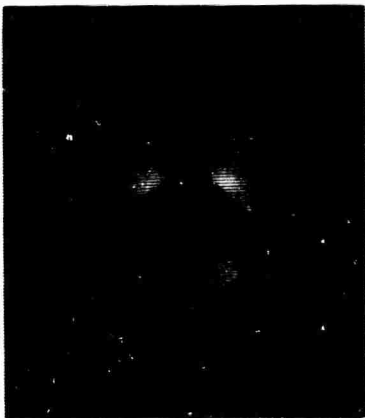


With Sample



Without Sample

Figure 20a - Interferometer Measurement of Optical Quality of Polymer



With Sample



Without Sample

Figure 20b - Crossed Glan-Thompson Prism Study of Birefringence

D. Preparation of Single Crystals

As noted above, single crystals of anthracene doped with naphthacene should be a promising organic laser material on the basis of the spectroscopy of the system. Some attempts were made to grow pure anthracene crystals and also to incorporate the naphthacene into the anthracene lattice. The anthracene used was the Kodak grade H-480 and was grown from the melt by a standard thermal gradient technique⁽³⁴⁾. In these experiments the anthracene was incorporated into an evacuated chamber which had been backfilled with 100 millimeters argon. It was found to be very difficult to grow anthracene with the proper orientation. In the experiments in which naphthacene was incorporated into the anthracene crystal, concentration gradients of naphthacene were found along the axis of the rod. The extent of this gradient depends very sharply on the growth rate which is ordinarily kept at about 1 mm per hour. Subsequently, some pure anthracene with the proper orientation was successfully grown. However, the level of effort required to grow a single crystal of anthracene in an appropriate size, orientation, and with the correct concentration of naphthacene was deemed too large a program for the current contract. As a result, further attempts to grow anthracene single crystals suitable for an organic laser rod were suspended.

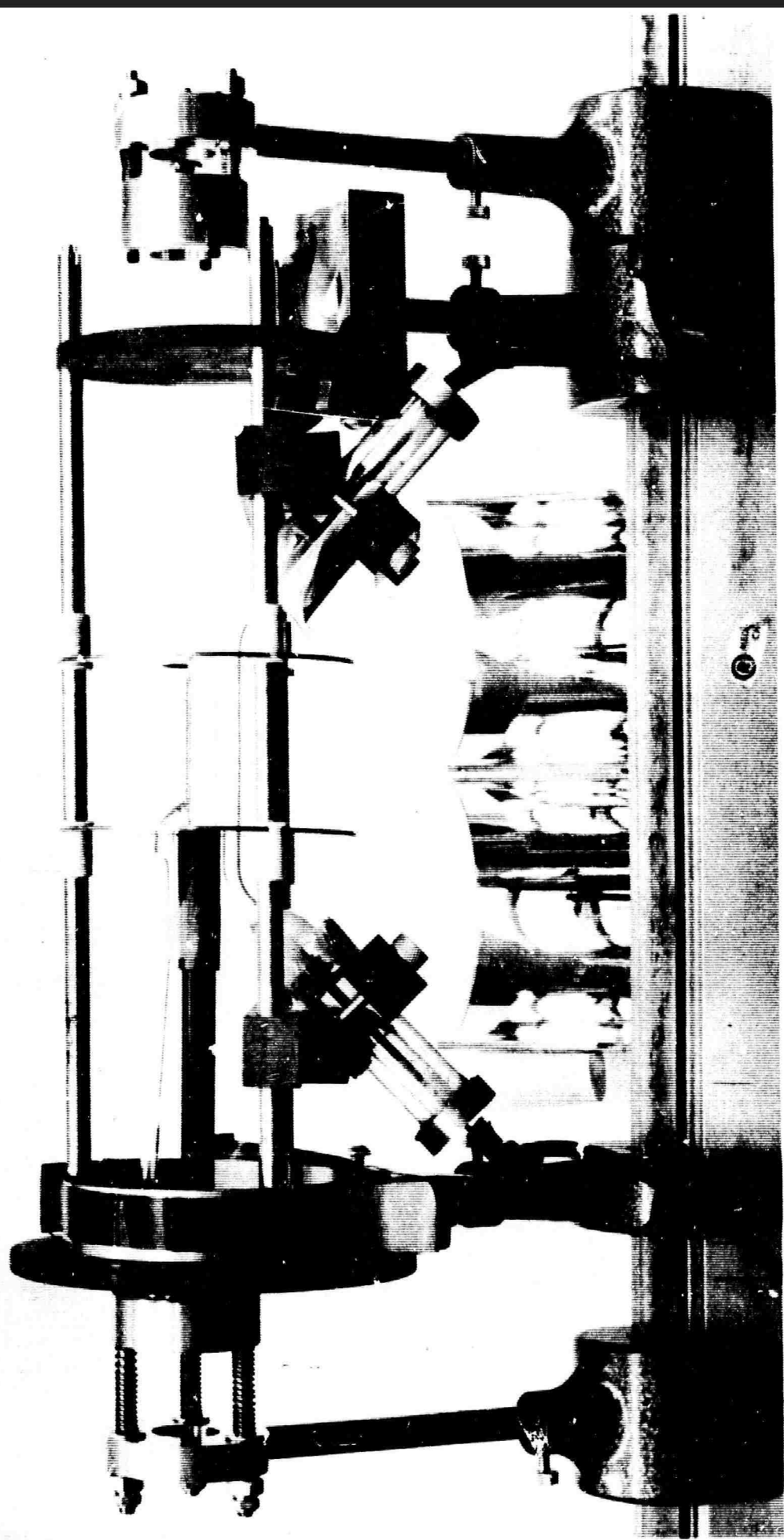
IV. DEVICE CONSIDERATIONS

A. Optical Pumping Systems

One of the major problems in the development of an organic laser employing fluorescent organic compounds is the generation of sufficient peak power in a short time. Several approaches to this problem have been attempted. Briefly stated, the threshold for these materials would require an absorbable photon flux of about 10^{23} photons per second into a volume corresponding to a sample 3" long and 1/4" in diameter.

1. Conventional Xenon Pumping Systems

The lamp system first attempted was aimed at modifying a conventional xenon lamp system to yield a pump pulse duration of less than 10 microseconds with an appropriate input energy of about 200 joules. For pulses of this length, relatively small capacitors must be used which will have a self-resonant frequency of about 200 KC. A five microfarad-20 KV GE type 14F 322 capacitor was used. Because the voltages used exceeded the breakdown potential of the lamps, a GE type GL7703 ignitron was employed as a switch. A variety of series inductances up to about 0.5 microhenries were employed in order to match the impedance of the driving circuit to that of the lamp. Several commercial xenon lamps and some custom lamps were tested but they could not withstand the shock waves generated. A lamp was built in this laboratory which was able to withstand the shock waves produced under these conditions. A photograph of this lamp in an optical cavity is shown in Figure 21. The electrodes were made of barium impregnated tungsten whose tips were ground to a hemispherical shape to reduce the shock wave input and to allow the hot expanding gas to carry sputtered materials to the region behind the electrodes. The ends of the lamp were bent at 45° to allow close optical coupling to the sample in the pseudo-elliptical cavity. Baffles made of several layers of 100 mesh stainless steel wire screen were located



EXPERIMENTAL XENON DISCHARGE LAMP ON A LASER TEST SETUP
FIGURE 2I

half way between electrode tip and end of the lamp. The re-entrant ends were potted with lead in a brass cup to dampen shock impact vibrations. The total arc length was 4" long with a 6 millimeter diameter discharge. The lamp was filled with 60 cm xenon after appropriate degassing. An EG and G FX-45 lamp was used to compare the brightness and efficiency for longer pulses. The bent lamp showed slightly greater brightness. A maximum peak power (measured at the half power points) of 43 megawatts (300 joules, 7 microsecond width) was discharged into this lamp. Because of the properties of the fluorescent molecules, the lamps' full peak power could not be utilized in pumping the liquids because the pulse was too long (see Section V). It was used to pump the rods formed from the polymer.

In considering generation of a shorter pulse (of about 400 nanoseconds or less), several questions immediately arise; (a) what types of capacitors are suitable to obtain such short pulses?, (b) will the efficiency and brightness of the xenon lamp or a lamp filled with other gases be maintained under these short pulse conditions?, (c) what techniques can be used to match the impedance of the driving circuit to that of the lamp (since the ordinary technique of adding a series inductance would lengthen the pulse time)?, (d) the need for an extremely fast, low-loss, high voltage switch.

The capacitor problem was attacked first. If a peak power of the order of 100 megawatts is desired in a 400 nanosecond pulse, the stored energy needs to be 40 joules. The resonant frequency of the capacitor must be at least 5 megacycles, and therefore, a low capacitance, high voltage capacitor is needed. Several commercial capacitors in the range 0.01 to 0.1 microfarads were tested at voltages up to 20 KV. The distributed inductance in each of them was too high and as a result the light pulses generated were much too long. Under a previous contract with the AEC, a series of high dielectric-constant, high dielectric-strength ceramic materials were investigated as energy storage capacitors. The details of this general class of non-piezoelectric barium-strontium

titanates can be found elsewhere⁽³⁵⁾. The dielectric constants of these materials can be as high as 4000 with field strengths of 400 volts per mil having been observed in some materials. It was decided to make capacitors from these materials in a form of a cylinder so as to minimize the distributed inductance. These capacitors proved to be highly successful for generating pulses from 125 to 350 nanoseconds duration depending on the lamp used. The properties and preparation most successful ceramic capacitors used are described in the Appendix. One capacitor was 0.016 microfarads and the other was 0.115 microfarads. The latter capacitor had a field strength of at least 150 volts per mil (30 KV) which corresponds to a stored energy of 50 joules.

Several types of lamps have been considered as potential optical pumps to use in developing the shorter pulses required. It was decided to use a lamp body corresponding to the GE FT-91 lamp. This lamp body was then filled with a variety of gases which were as follows;

- (a) Xenon-30 cm.
- (b) Xenon-2.5 cm.
- (c) Xenon-30 cm., Iodine-2.0 cm.
- (d) Helium-30 cm.
- (e) Hydrogen-4.0 cm.
- (f) Air-2.5 cm.
- (g) Air-10 cm.
- (h) Nitrogen-2.5 cm.

The pressures were chosen to insure a high voltage breakdown for the lamp of about 7 KV and, hopefully, to minimize the impedance. The switches used were EG and G GP-17 spark gaps used in series to provide the necessary hold-off voltage. The dynamic impedance of these switches is a few milliohms.

The air-filled lamps yielded the shortest pulses when used in conjunction with the ceramic capacitors. These pulses were as short as 125 nanoseconds, but a factor of 15 less bright than the xenon (30 cm.)

pulses. The xenon pulses have a full width at half maximum of 350 nanoseconds. A major portion of the time was spent in making surface brightness measurements to determine if the lamps were operating efficiently. The brightness standard used for comparison was the same lamp pumped from a lower power, shaped pulse circuit yielding a light pulse of 30 microseconds duration. (This discharge condition typically yields for a 30 cm xenon lamp-radiative efficiency of about 50%). The brightness was measured with and without a narrow band pass filter centered at 4100 Å. Although the apparent peak power (measured from the pulse width and the stored energy) of the shorter pulses was 50 fold higher than for the long pulse, the brightness of the short pulse was only a factor of 2 greater, indicating that the efficiency of such lamps is not particularly high with the short pulses. Measurements of the spectral output of the 30 cm xenon lamp showed an equivalent black body temperature of about 7500°K.

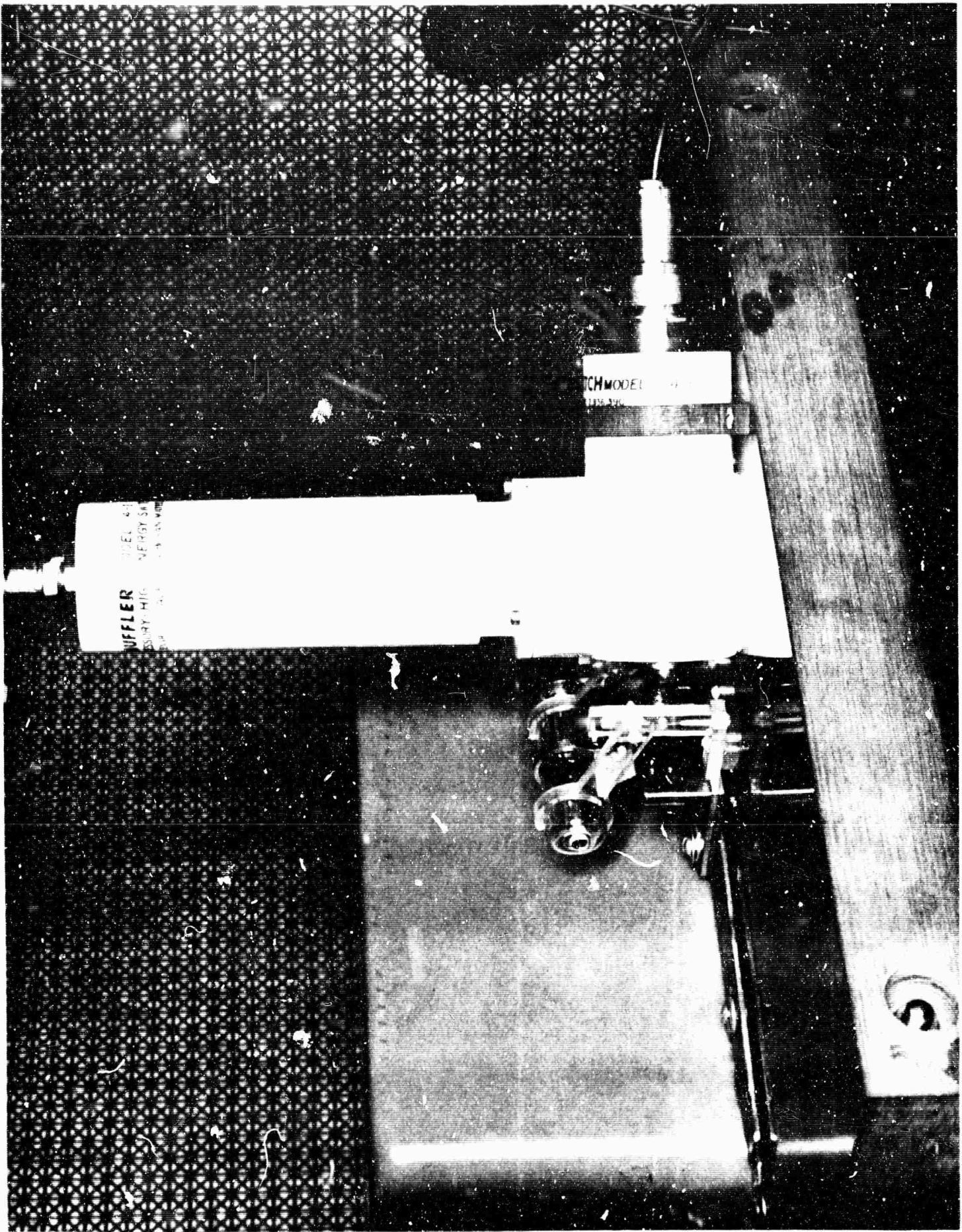
Attempts were made to increase the brightness of the short pulse lamps by improving the impedance match between the driving circuit and the lamp body. A DC "keep-alive" increased the brightness by a factor of 2 with perhaps a slightly improved rate of rise of the light output. Double pumping experiments were attempted to see if the type of high brightness results reported by Emmett and Schawlow could be obtained using the very short pulses. The long pulses were 30 microseconds with an energy of about 10 joules while the short pulse lasted about 350 nanoseconds and had a stored energy of 3-4 joules. The brightness of this double pump system did not show any significant improvement over the DC "keep-alive" results. Varying the time at which the short pulse was allowed to dump into the lamp did not produce significant changes. Varying the energy discharged into the lamp also did not produce significant improvement.

2. Theta-Pinch Lamps

Another possible pumping source is the argon theta-pinch lamp work described recently (as modified for laser pumping) by Feldman and coworkers⁽³⁶⁻³⁸⁾, at Carnegie Tech. Feldman's pumping system consists of a clam shell capacitor (40 KV, 1 microfarad) connected through an air-gap switch to a brass strap of about 1/4" cross section curved to form a circular loop of 1" diameter. Within the loop he places a toroidal bottle with the laser rod at the center. The bottle contains any of the rare gases (usually argon) to a pressure of a 1 to 100 millimeters. When the switch is triggered, the large induced electrical field ionizes a channel in the gas in the toroidal bottle. Enormous currents are induced for a very short period of time. Typical current densities reported by Feldman are 5×10^5 amperes/cm², power inputs to the gas reach 4×10^8 watts and the total energy dissipated in his lamps have been as high as 400 joules. The pulse length is about 1 microsecond. The lamp has been operated repetitively at rates as high as 60 cycles per second and as long as 5 minutes at 30 cycles per second using only natural convection for cooling. Thus, the lamp is apparently exceptionally effective at re-radiating the input energy.

An optical pumping system based on Feldman's design was constructed in this laboratory. It utilized a 0.9 microfarad, 50 KV clam shell capacitor (GE 14F-756C2) in conjunction with high current pressurized switch (obtained from Cooke Engineering Company, Alexandria, Virginia) and a toroidal bottle (containing 2.5-3.0 mm argon) of the same dimensions (1 1/8" O.D., 5/16" I.D. 3" long) which Feldman used. A photograph of this apparatus is shown in Figure 22.

In order to check on the earlier, rather crude results of Feldman⁽³⁹⁾ on the spectral properties of argon theta-pinch lamps, a series of measurements were made on the spectral properties of the lamp which we had built.



ARGON THETA PINCH LAMP

FIGURE 22

A dual-grating, 2-meter Bausch and Lomb spectrograph was the basic component of the measuring system. The lamp was operated at 36 KV for these measurements and was a distance of 153 cm from the entrance slit of the spectrograph. A 1 mm entrance slit (corresponding to 4 Å dispersion) was used and Type 103-0 Kodak film plate was employed. A Hg-Cd source was used to calibrate the wavelengths. The region covered was 2700-5700 Å in 1000 Å sections. The plate densities were recorded on a Leeds and Northrup recording densitometer and are shown in Figures 23-25. Note that the plate density scale is different for the wavelength region from 4900 to 5500 Å. The response of Type 103-0 plates is such that the sensitivity vs. wavelength curve is essentially flat over the region 3000-4700 Å. Due to an error in moving the grating, the region 3600-3775 Å was missed. There are eleven lines of argon I of good intensity in this region and one line of un-ionized argon so that some information was lost. Time and money did not permit repeating the measurements for this data, since they were performed in another laboratory. In interpreting the spectroscopic data, plate densities in excess of 1.7 or less than .05 should not be regarded as being particularly accurate. Between these regions the relative intensity data should be good.

The result of this measurement is the general confirmation of Feldman's observation that a continuum exists with a very large number of spectral lines superimposed on top of it. The continuum peaks near 3800 Å in our data. The most interesting feature of this new data show that almost all of the lines present are dispersion-limited to 4 Å in width. A measurement of the total energy radiated with these lines is therefore not possible.

At the lamp pressure employed (2.5 mm), pressure broadening should not be significant and this data confirms this observation. A tabulation of all of the lines with respect to their origin was started but not completed. However, the higher ionized states of argon are present and apparently in high enough concentrations to significantly contribute to the brightness of the source.

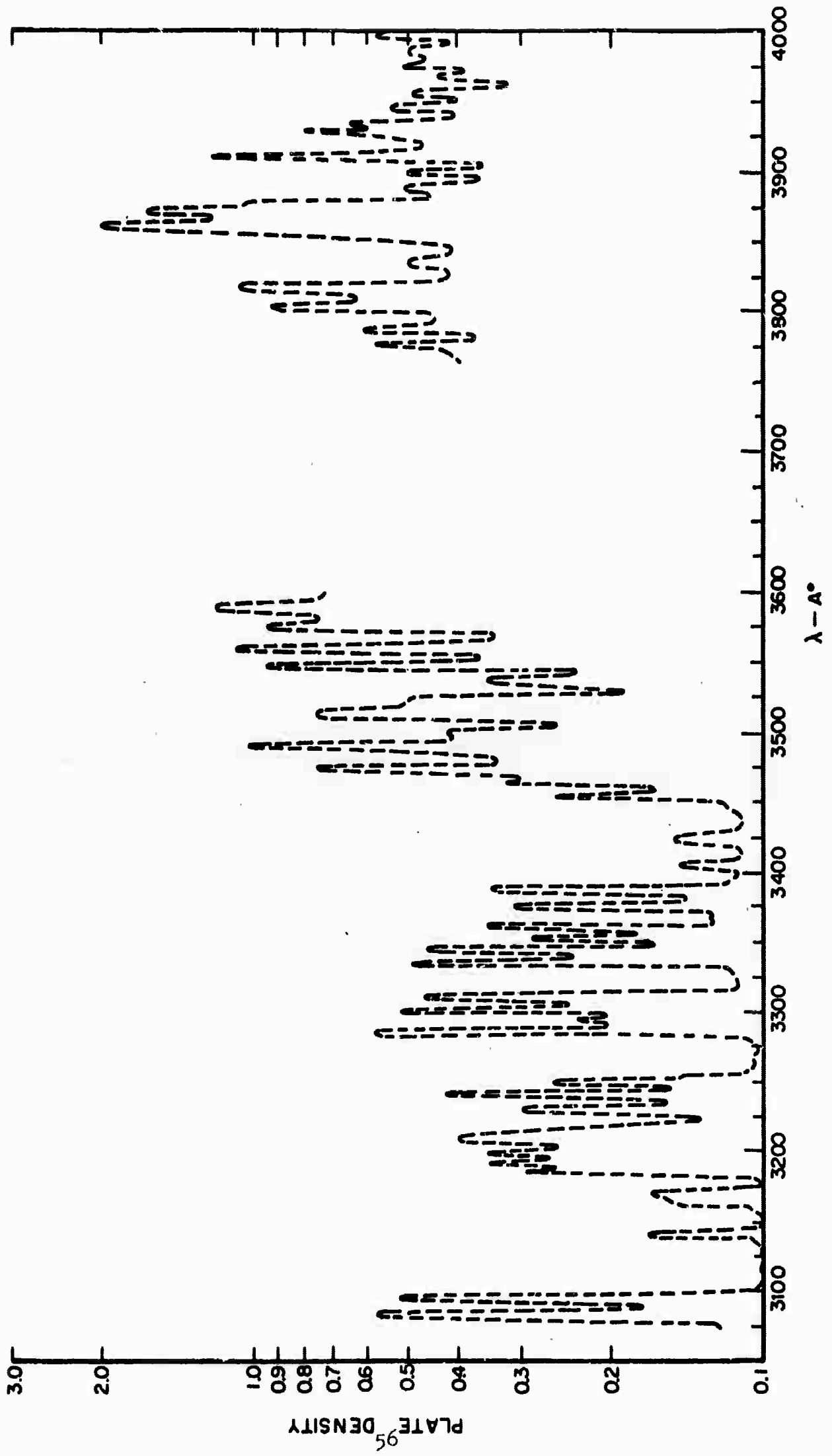


FIGURE 23 SPECTRAL OUTPUT OF ARGON THETA PINCH LAMP (2.5 mm. PRESSURE)

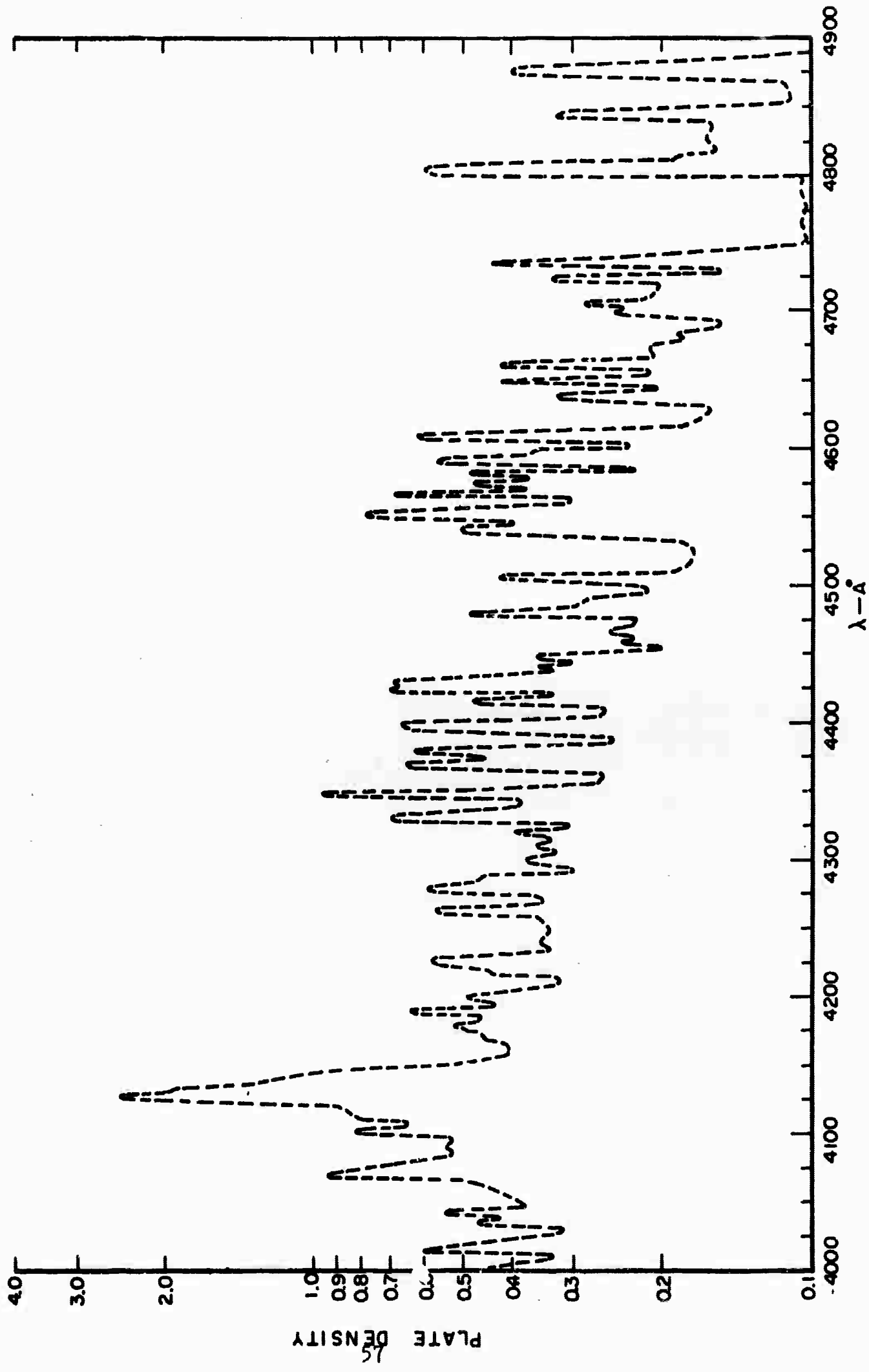


FIGURE 24 - SPECTRAL OUTPUT OF ARGON THETA PINCH LAMP (2.5mm PRESSURE)

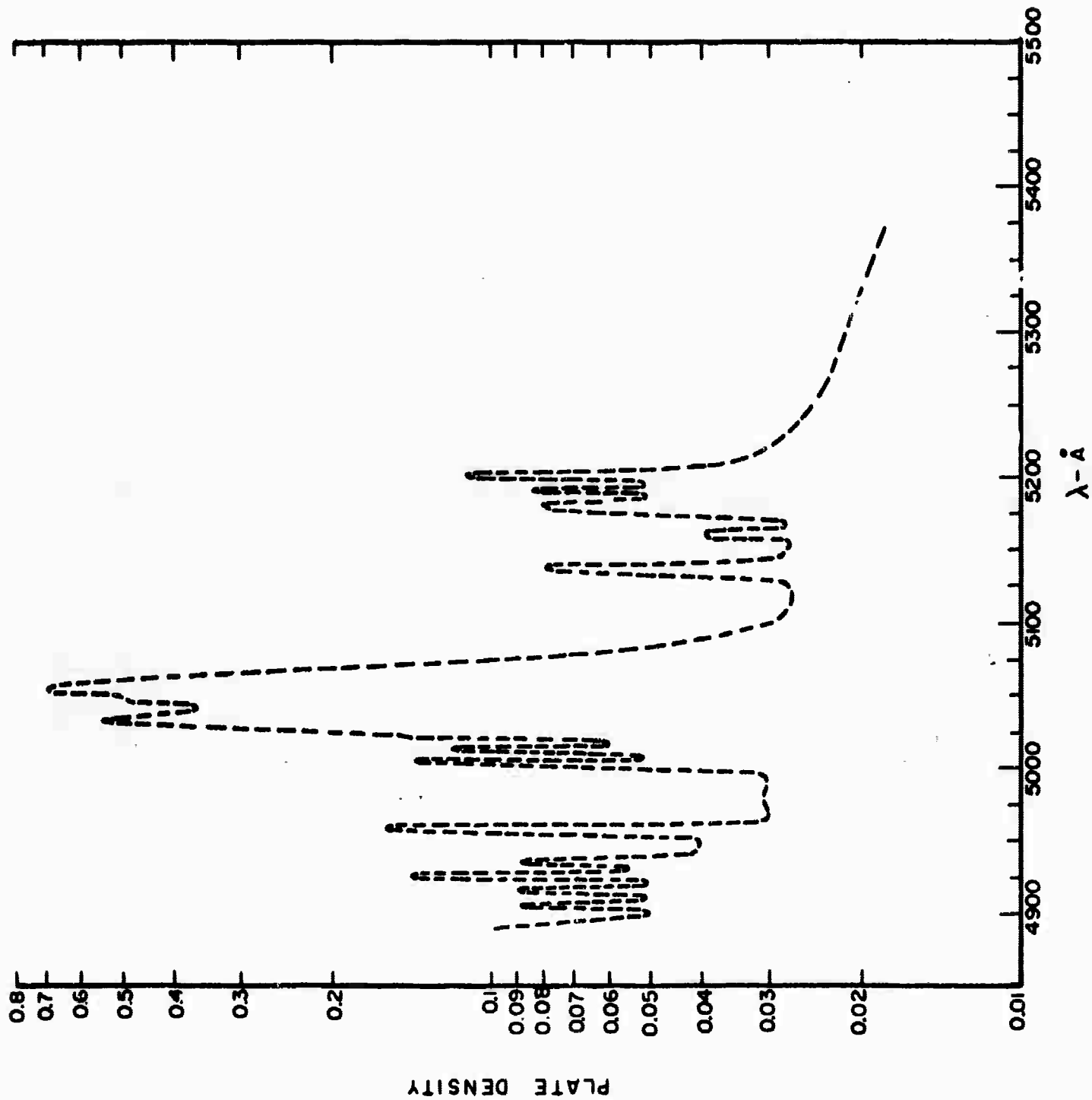


FIGURE-25 SPECTRAL OUTPUT OF ARGON THETA PINCH LAMP (2.5 mm PRESSURE)

At the lamp pressure employed (2.5 mm), pressure broadening should not be significant and this data confirms this observation. A tabulation of all of the lines with respect to their origin was started but not completed. However, the higher ionized states of argon are present and apparently in high enough concentrations to significantly contribute to the brightness of the source.

The brightness of the lamp is important in order to establish if it will develop enough radiated power within the pumping bands through each threshold for the organic fluorescent materials. A direct measurement of the spectral irradiance was made by calibrating the system against a GE 7458-2 standard lamp which had been directly compared with an NBS standard. For this measurement, a set of eight photomultipliers replaced the photographic plate on the spectrograph. The slits for the photomultipliers were 7 mm wide (28 Å) and were separated on centers of 35 mm (140 Å) and an entrance slit with 1 mm was used. More detailed data on the instrumentation used can be found elsewhere⁽⁴⁰⁾. The photomultipliers were operated identically for the two measurements except that different calibrated load resistors were used to correct for the four orders of magnitude difference in brightness between the calibration and the theta-pinch lamp source. Voltages for the calibrating lamp were read on a voltmeter while the theta-pinch lamp peak brightness was read off the oscilloscope trace.

The spectral irradiance, $S(\lambda)$, in watts per cm^2 per micron was measured using the slits of 7 mm. Since both the calibration source and the lamp were used with the fixed slits of 7 mm, the relative brightness of the source is given by

$$S(\lambda)_{\text{source}} = S(\lambda)_{\text{standard}} \times \frac{5.10 \times 10^6}{5.10 \times 10^2} \times \frac{V_{\text{lamp}}}{V_{\text{standard}}}$$

where the resistances used for the two different measurements have been put in as a multiplier. At 3795 Å, the standard source irradiance was given from the calibration as 6.96×10^{-4} watts per (cm^2 micron) while the voltage ratio $V_{\text{lamp}}/V_{\text{standard}} = 0.70$, therefore,

$$\begin{aligned} S(\lambda)_{\text{source}} &= 6.96 \times 10^{-4} \times 0.7 \times 10^4 \\ &= 4.8 \text{ watts cm}^{-2} \text{ micron}^{-1} . \end{aligned}$$

The average spectral radiance (in watts per (cm^2 micron)) of the lamp is given by multiplying the spectral irradiance by the square of the distance of the lamp from the slit divided by the projected area of the lamp. For our measurements, the distance was 153 cm and the projected area was 1.65 cm^2 . Thus, the spectral radiance at the maximum (3795 Å) was

$$4.8 \times \frac{(1.53 \times 10^2)^2}{1.65} = 5.9 \times 10^4 \text{ watts cm}^{-2} \text{ micron}^{-1} .$$

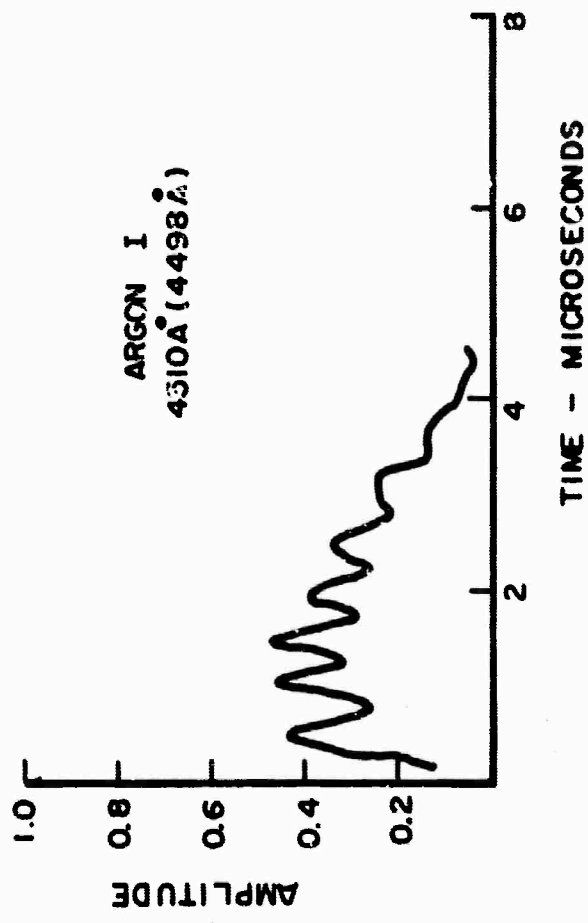
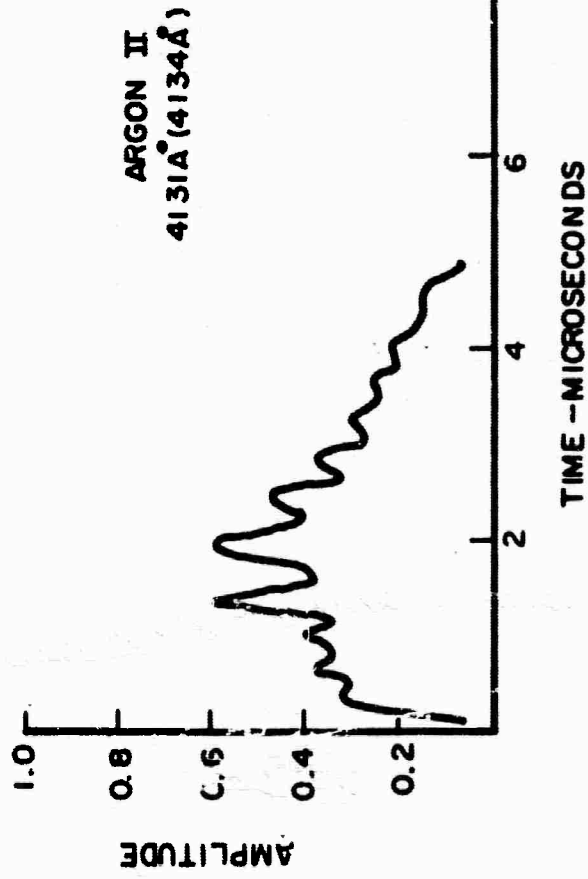
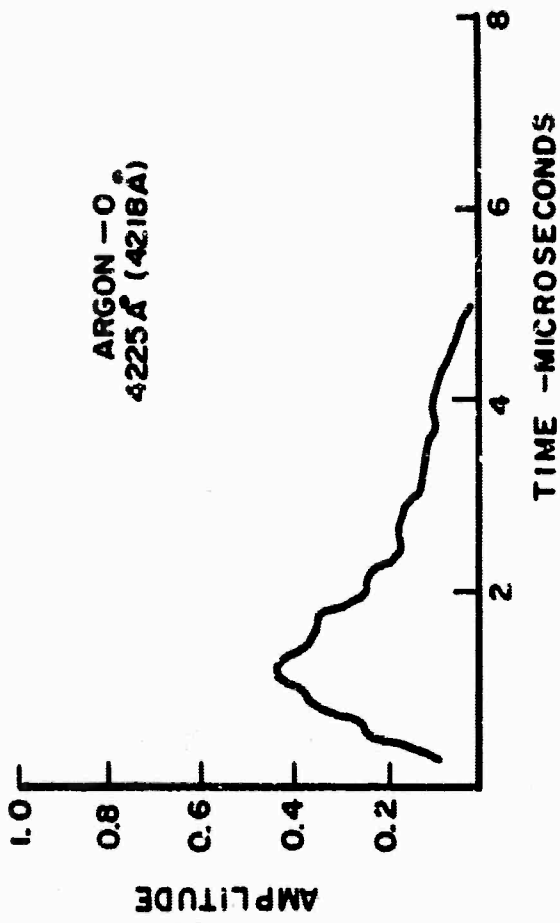
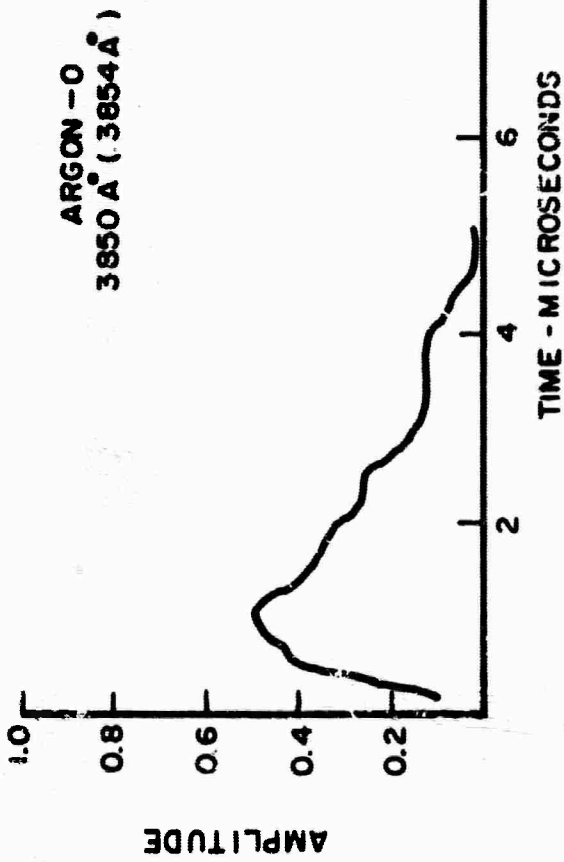
For a blackbody radiating at its maximum wavelength and whose spectral radiance is 5.9×10^4 watts per (cm^2 micron) the temperature would be 8600°K and the radiation would have its maximum at about 3400 Å. In view of the accuracy of the data, these results are in reasonably satisfactory agreement but it should be pointed out that possible errors in the measurement preclude definitely assigning the origin of the continuum to blackbody radiation.

A measurement of the total radiated power, and thus the efficiency of the lamp, is not really possible on the basis of these measurements. This is due to the fact that the spectral lines are for the most part much narrower than the 4 Å dispersion used for the measurements. In addition, the lamp does not radiate uniformly, but is most intense near the coupling loop and falls off towards the end of the toroidal lamp.

If we consider as an assumption that the effective radiating area is one-third of the total 60 cm^2 and if we consider that the peak power of the lamp is given by $1/2 CV^2/\tau$, where τ is the full width of the pulse at

half maximum, then at the 36 Kv (0.9 μ f) we have a peak power of about 195 megawatts. For 20 cm² effective radiating area, the input electrical power is 1×10^6 watts/cm². For blackbody continuum at 8600°K, the system radiates 3.1×10^4 watts per cm² for an emissivity of one. This gives an overall efficiency of 3% for conversion of electrical energy to continuum radiation. Since the spectral lines contribute heavily, the real efficiency is considerably above this figure. In addition, considerable circuit losses in the switch and the capacitor will prevent the full energy from being dissipated into the lamp and so the real efficiency of the lamp is increased even further quite probably.

A series of studies were performed on the lamp in an effort to study the time relationships between the various species radiating in the lamp. This is important to understand whether or not a quasi-equilibrium exists between the various ionized species of argon. These measurements were taken with the photomultiplier units previously described. The results were fed to the two Type 555 Tektronix oscilloscopes with dual channel inputs. Since the pulses were faster than the chopping rates available, only four channels (on two oscilloscopes) could be monitored at one time. After two flashes the photomultiplier units were shifted 7 mm to study the next portion of the spectrum. Using this technique it was possible to measure the time-resolved output over the range 3700-4700 Å. Some data obtained are plotted in Figure 26. Only times above and below each other should be compared since the left and right hand pairs were taken with different flashes. The relative amplitudes have meaning only with one plot. The symbol 3850 Å (3854 Å) refers to the first number to the center frequency of the radiating species and the second number to the center wavelength of the 7 mm (28 Å) wide photomultiplier slit. The un-ionized argon lines at 3858 Å and 4225 Å are of moderate intensity and also continuum is evident in these traces. The argon I and II outputs follow the electrical ringing in the circuit while the un-ionized



TIME DEPENDENT OUTPUT OF VARIOUS SPECIES
FIGURE 26

argon and the continuum exhibit only a very small variation with respect to the circuit characteristics.

We can interpret this type of data to mean that no quasi-equilibrium exists between the ionization states and the continuum while the un-ionized argon may be in equilibrium. The failure of the un-ionized argon follow the circuit characteristics is evidence that it is not participating in power coupling between the electrical loop and the plasma.

B. Fabry-Perot and Confocal Resonant Cavities

The resonant optical cavity can be formed in a number of ways using a variety of reflector materials. One important criterion for threshold in a four-level system is that the reflectivity of the end mirrors be kept as high as possible. Silver mirrors are unsatisfactory in this respect since they have a maximum reflectivity at 4700 Å of 97.5%. Other metallic coatings have even lower reflectivities in this region. Dielectric coatings are superior in this respect and are used to form the resonant cavity. The dielectric coatings presently used were made by Perkin-Elmer Corp. especially for us and have greater than 99% reflectivity at 4700 Å extending over a 10%-15% bandwidth and one set of mirrors covered all of the compounds given attention in this study. Optical flats and confocal mirrors are equipped with these coatings. The confocal arrangement has the advantage that the optical alignment need by much less precise to obtain reproducibly low thresholds. The radius of curvature of the confocal mirrors used was 5 1/2".

Antireflection coatings on the ends of the rod become an important consideration for reducing the threshold requirements when the scattering losses are reduced to the order of 0.02 per cm or less. For a material of refractive index 1.50 such as is the case for a polymer rod, the perfect quarter wavelength thickness antireflection coating should have a refractive index of 1.22. However, a quarter wave magnesium fluoride film (refractive index = 1.37) would reduce the Fresnel reflection losses from 4% per surface to 0.4% per surface.

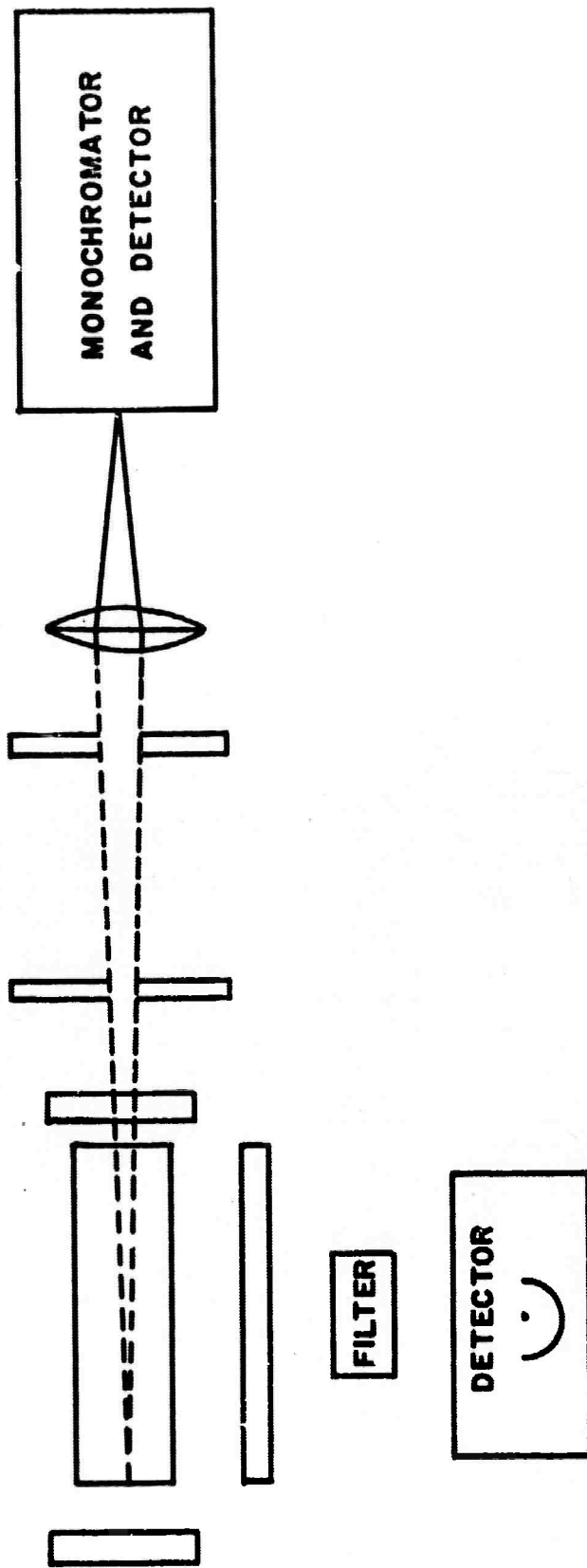
V. RESULTS OF OPTICAL PUMPING EXPERIMENTS

Optical pumping experiments with the resonant cavity in place have been made with the long light pulses generated by the bent lamp and power supply described in Section IV-A-1. Because the life time of the fluorescence in these materials is a factor of 1,000 shorter than the pump pulse duration, an exact steady state exists and the fluorescence intensity at any point in time represents the true density of excited states.

It was decided to observe the pump pulse and the fluorescence pulse simultaneously to look for non-linearities in the fluorescence output. The bent lamp (see Section IV-A) was used to pump the samples. A solution of 6×10^{16} molecules/cm³ of perylene in benzene at room temperature was used for these experiments. The experimental arrangement used is shown in Figure 27. A photocell was used to monitor the pumping radiation as a function of time. A filter which passed only the pumping band of the fluorescent material was placed in front of the photocell. The pump pulse thus represents the true rate of absorption of photons by the perylene molecules. A 500 mm. focal length grating monochromator (resolution 16 Å per mm) was fitted with an RCA 1P28 or RCA 7265 photomultiplier and monitored the fluorescence output along the axis of the resonant optical cavity. For most of these experiments the resonant cavity was formed using dielectric 4700 Å reflectors in a Fabry-Perot structure or in a hemispherical cavity. Appropriate apertures limited scattered pump radiation to an insignificant fraction of the fluorescent output. The half angle of the cone of observation was 2 minutes of arc.

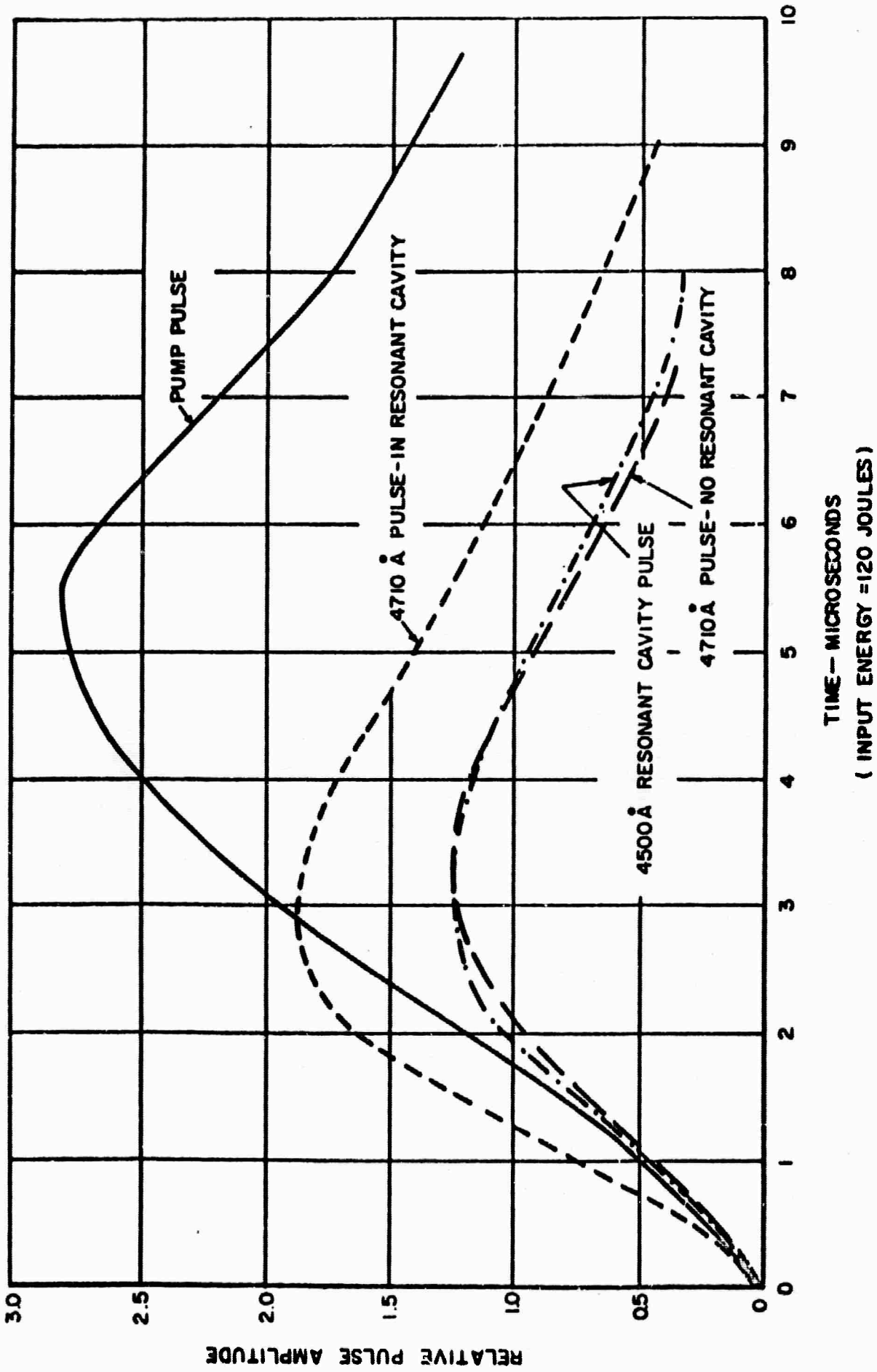
Measurements were made at various wavelengths along the fluorescence peaks and in regions where the fluorescence is negligible. The results are as follows:

- (a) The fluorescence at 4710 Å (see fluorescence spectrum in Figure 3) rises faster than the pumping radiation with the resonant cavity in place in both the liquid and plastic samples when the peak power of the pumping system is increased to a certain point. When the resonant cavity is destroyed by removing one mirror, this effect can no longer be seen. Figure 28 shows plots of the observed effects.



OPTICAL SYSTEM FOR FLUORESCENCE GAIN MEASUREMENTS

FIGURE 27



FLUORESCENCE OF PERYLENE IN BENZENE SOLUTION AT VARIOUS WAVELENGTHS

FIGURE 28

- (b) The increase in fluorescence intensity mentioned in part (a) occurs only at wavelengths corresponding to the four-level transition. At 4500 Å (in the three-level fluorescence band) the effects are not observed with or without the resonant cavity (see Figure 28).

As estimate of the maximum excess fluorescence intensity shows it to be about 5% per cm. Since the fluorescence lifetime is a factor of 1,000 shorter than the pump pulse duration, the excited singlet state population is in an exact steady state at any time. Thus, there is no possibility of excess fluorescence being generated by the pumping system. We believe, tentatively, that the excess fluorescence represents gain taking place due to stimulated emission by the perylene in the benzene solution.

The premature decay of the fluorescence is probably due to a depletion of the molecules available for pumping the singlet states because of the gradual build-up of triplet states, which have a relatively long relaxation time (10^{-5} to 10^{-4} seconds). This build-up occurs because the quantum efficiency of fluorescence for perylene in benzene is only about 96%. The other 4% represents conversion to the lowest-lying long-lived triplet state. Since each molecule is pumped on the average of 1,000 times during the pump pulse, the triplet state can build up to appreciable levels at high pumping rates. As a result the full peak power of this pumping system could not be utilized.

Attempts to achieve gain by pumping the liquids samples with the theta-pinch lamp were unsuccessful. Perylene, 9-amino-acridine, 9-methylanthracene and 9,10-diphenylanthracene contained in the polymer were pumped in both the xenon lamp system and in the argon theta-pinch lamp system. No gain could be detected using the xenon lamp system. Forty-three megawatts was the highest peak power used. The theta-pinch lamp was exceedingly noisy and prevented accurate gain measurements for being performed. With this lamp, one looks simply for a spatially coherent beam or for a large increase in intensity. None was found although the peak powers employed reached values up to 250 megawatts.

VI. APPENDIX

Preparation of Ceramic Capacitors

Under a previous contract with the AEC⁽³⁵⁾, this laboratory developed a series of ceramic capacitors employing high dielectric-constant, high dielectric-strength materials for application as energy storage units. Since the capacitance per unit volume with these materials is high, it was thought that the fabrication of coaxial cylinders of these materials would yield a capacitor with very low distributed inductance, which would enable very short pulses to be obtained. Such a material must exhibit no piezoelectric characteristics as it would disintegrate upon rapid discharge due to rapid volume change.

Barium titanate and strontium titanate are well known for their high dielectric constants. Barium titanate has a high dielectric constant but it is also piezoelectric at room temperature. Strontium titanate has a somewhat lower dielectric constant, but also a Curie temperature far below room temperature. A mixture of 65% barium titanate and 35% strontium titanate by weight has been used extensively in industry as a capacitor material. The Curie temperature is just below room temperature and a high dielectric constant is obtained. However, uniform density and controlled grain size are of the utmost importance in obtaining good electrical characteristics. In order to obtain these good characteristics a very pure starting material must be employed along with careful techniques of preparation and controlled firing conditions. Two compositions were chosen for the present work. The designations are DL85 and K1200⁽³⁵⁾. The latter material is a barium titanate with bismuth stannate added to reduce the piezoelectric character of the barium titanate.

The DL85 mixture was weighed and mixed by dry ball milling for 16 hours. It was broken up and calcined at 1200°C for two hours. It was then broken up again to 4-mesh particle size and dry ball milled for four hours to a 20-mesh particle size. Water was added and it was ball milled again for 16 hours. Hyform 1214 emulsion was added and it was dried at 70°C for two hours. It was then made into a 20-mesh particle size again.

It was then pressed isostatically in the form of a cylinder at 3000 psi. The final firing was accomplished by raising the temperature to 1175°C in a forced air atmosphere. From 1175-1350°C an oxygen atmosphere was used. It was then soaked at 1450°C for two hours in a forced air atmosphere. An argon atmosphere was then used and the sample cooled in this environment. The cylinder was then ground to the final dimensions of 5" length, 2-1/4" outside diameter and about 0.200" wall thickness.

Dupont 4731 silver paste was applied inside and outside of the cylinder as an electrode and fired 720°C for one hour. Two to three layers produce a uniform electrode possessing extremely low resistance. Silver electrode tabs were then applied with Eccobond 56C conducting epoxy. The resistivity of this epoxy is 10^{-4} ohm-cm. With this operation the capacitor is complete. A measured capacitance of 0.115 microfarads for the DL85 cylinder was obtained corresponding to a dielectric constant of 3850-3900. The K1200 material was made for us employing similar techniques by the Electronics Ceramic Unit of General Electric, Syracuse, New York.

To avoid corona at the edges, the cylinder was immersed in a silicone oil when used at voltages in excess of 10 KV. The pulses obtained from this capacitor are described in Section IV-A.

VII. BIBLIOGRAPHY

1. EG Brock, et.al., J. Chem. Phys., 35, 759 (1961).
2. AP Ivanov, Optics and Spectroscopy, 8, 183 (1960).
3. DJ Morantz, BG White and AJC Wright, Phys. Rev. Letters, 8, 23 (1962).
4. DJ Morantz, BG White and AJC Wright, J. Chem. Phys., 37, 204 (1962).
5. DJ Morantz, Optical Masers, pp. 491-501, Polytechnic Press, Brooklyn, N.Y., 1963.
6. A Lempicki and H Samelson, Appl. Phys. Letters, 2, 159 (1963).
7. F Wilkinson and EB Smith, Nature, 199, 691 (1963).
8. DL Stockman, KF Tittel and WR Mallory, (to be published).
9. M Kasha, Radiation Research Supplement, 2, 243 (1960).
10. P Pringstein, Fluorescence and Phosphorescence, pp. 441-444, Interscience Publishers, New York, 1949.
11. TH Forster, Fluorescenz Organister Verbindungen, Vandenhoeck U Ruprecht, Goettingen, 1951.
12. H Jaffe and M Orchin, Theory and Application of Ultraviolet Spectroscopy, John Wiley and Sons, Inc., New York, 1962.
13. A Yariv and JP Gordon, Proc. IEEE, 51, 4 (1963).
14. TH Maiman, Phys. Rev., 123, 1145, 1151, (1961).
15. DS McClure, J. Chem. Phys., 17, 905 (1949).
16. G Porter and MW Windsor, Proc. Royal Society, A245, 238 (1958).
17. J Fronk, Space Sciences Laboratory, General Electric Company, Valley Forge, Pa., Private Communication.
18. EJ Bowen and R Livingston, J. Amer. Chem. Soc., 76, 6300 (1954).

19. SJ Strickler and RH Berg, J. Chem. Phys., 37, 814 (1962).
20. EV Shpol'skii and RI Personov, Optics and Spectroscopy, 8, 172 (1960).
21. EJ Bowen, Trans. Far. Soc., 50, 97 (1954).
22. WR Ware and BA Baldwin, J. Chem. Phys., 40, 1703 (1964).
23. JB Birks and DJ Dyson, Proc. Roy. Soc , A275, 135 (1963).
24. E. Bowen and J. Sahu, J. Phys. Chem., 63, 4 (1959).
25. A Schmillen, Luminescence of Organic and Inorganic Materials, p. 36, John Wiley and Sons, Inc., New York, 1962.
26. DP Craig, Organic Crystal Symposium, Oct. 10-12, 1962, Ottawa.
27. RD Andrews and JF Rudd, J. Appl. Phys. 28, 1091 (1952).
28. RS Stein, Die Physik der Hochpolymeren, Ed. by Stuart, Part 9, p. 110 of Ch. 1, Vol. 4, Springer, Berlin, 1956.
29. EF Gurnee, J. Appl. Phys. 25, 1232 (1954).
30. RH Wiley and GM Brauer, J. Polymer Sci., 3, 455 (1948).
31. F. Pockels, Ann. der Physik, Serial IV, 7, 745 (1902).
32. JH Lambie and ES Dahmouch, Brit. J. Appl. Phys., 9, 388 (1958).
33. American Institute of Physics Handbook, p. 6-20, McGraw-Hill, New York (1957)
34. FR Lipsett, Can. J. of Phys., 35, 284 (1957).
35. Final Report, Contract No. AT (30-1)-1963 to the United States Atomic Energy Commission.
36. JM Feldman and JS Hitt, "Spectra of High Intensity Electrodeless Discharges in Rare Gases," American Physical Society Meeting, Edmonton, August 1963.
37. RH Brandewie, JS Hitt and JM Feldman, J. Appl. Phys. 34, 3415 (1963).
38. WT Haswell, JS Hitt and JM Feldman, IEEE, 52, 93 (1964).
39. JM Feldman, Proc. Laser Flash Lamp Symposium, San Francisco, Feb. 1964.
40. H. Koenig, Final Report on Contract NONR 4121(00) with Office of Naval Research, March 1964.